NASA Technical Memorandum 110161

Modeling of Aircraft Unsteady Aerodynamic Characteristics

Part 2 - Parameters Estimated From Wind Tunnel Data

Vladislav Klein and Keith D. Noderer
The George Washington University, Joint Institute for Advancement of Flight Sciences, Langley Research Center, Hampton, Virginia

April 1995

National Aeronautics and
Space Administration
Langley Research Center
Hampton, Virginia 23681-0001

SUMMARY

Aerodynamic equations with unsteady effects were formulated for an aircraft in one-degree-of-freedom, small-amplitude, harmonic motion. These equations were used as a model for aerodynamic parameter estimation from wind tunnel oscillatory data. The estimation algorithm was based on nonlinear least squares and was applied in three examples to the oscillatory data in pitch and roll of a 70° triangular wing and an X-31 model, and in-sideslip oscillatory data of the High Incidence Research Model 2 (HIRM 2). All three examples indicated that a model using a simple indicial function can explain unsteady effects observed in measured data. The accuracy of the estimated parameters and model verification were strongly influenced by the number of data points with respect to the number of unknown parameters.

SYMBOLS

a	parameter in indicial function
b	wing span, m
b_1	parameter in indicial function, 1/sec
C_l, C_m	rolling- and pitching-moment coefficient
C_N	normal-force coefficient
$C_{N_\alpha}(t)$	indicial function
$\mathrm{Cov}\left(\hat{\boldsymbol{\theta}}\right)$	covariance matrix of estimated parameters
c	parameter in indicial function
$\bar{c}$	wing mean aerodynamic chord, m
$F_\alpha(t)$	deficiency function
J	cost function
k	reduced frequency, $k = \frac{\omega \ell}{V}$
ℓ	characteristic length, $\ell = \frac{\bar{c}}{2}$ or $\ell = \frac{b}{2}$, m
$\boldsymbol{M}$	matrix in normal equations
m	number of frequencies
n	number of angles of attack
p, q	roll rate and pitch rate, rad/sec
S	wing area, m^2
s^2	variance
s	a.) standard error b.) parameter in Laplace transform (Appendix A)
T_1	time constant, sec
t	time, sec
u, v	aerodynamic derivatives in model for in-phase and out-of-phase component of oscillatory data, respectively
$\bar{u}, \bar{v}$	in-phase and out-of-phase components of oscillatory data, respectively
z_u	term in model equation (6), $z_u = \frac{\tau_1^2 k^2}{1+\tau_1^2 k^2}$
z_v	term in model equation (7), $z_v = \frac{\tau_1}{1+\tau_1^2 k^2}$

α	angle of attack, rad or deg
β	sideslip angle, rad or deg
δ_c	canard deflection, deg
$\boldsymbol{\theta}$	vector of unknown parameters
τ	time delay, sec
τ_1	nondimensional time constant, $\tau_1 = \dfrac{V}{b_1 \ell}$
ϕ	roll angle, deg
ω	angular frequency, rad/sec

Superscript:

$\hat{}$	estimated value

Superscript over aerodynamic derivative:

$\bar{}$	oscillatory data in pitch or roll
$\tilde{}$	oscillatory data in heave or sideslip

Subscript:

A	amplitude
0	nominal value

Matrix exponent:

-1	inverse matrix
T	transpose matrix

Aerodynamic derivatives:

$$C_{A_a}(\infty) = \frac{\partial C_A}{\partial a} \text{ for } A = l, m, \text{ or } n \text{ and } a = \frac{pb}{2V}, \frac{\dot{p}b^2}{4V^2}, \frac{q\bar{c}}{2V}, \frac{\dot{q}\bar{c}^2}{4V^2}, \alpha, \beta, \text{ or } \frac{\dot{\beta}b}{2V}$$

INTRODUCTION

Reference 1 presents a short theoretical study of aircraft aerodynamic model equations with unsteady effects. In one of the examples in this study, a formulation of unsteady aerodynamics is applied to small-amplitude, one-degree-of-freedom harmonic motion of an aircraft about one of its body axes. The mathematical models developed can be directly used in the analysis of wind tunnel data obtained from forced oscillatory tests. During these tests, a model is forced to oscillate in the tunnel airstream about any single model body axis at a specified angular frequency and amplitude. From the measured aerodynamic forces and moments, the in-phase and out-of-phase components of the aerodynamic coefficients are obtained (see reference 2). It has been a long-standing practice to analyze the oscillatory data by formulating the aerodynamic model equations with constant parameters known as stability derivatives. In this formulation, the in-phase component is a combination of a static derivative (such as C_{m_α}) and a rotational acceleration derivative (such as $C_{m_{\dot{q}}}$) whereas the out-of-phase component is a combination of a purely-rotary derivative (such as C_{m_q}) and a translation acceleration derivative (such as $C_{m_{\dot{\alpha}}}$).

The results from forced-oscillatory tests with a given amplitude and at a given angle of attack show that the resulting combinations of derivatives very often depend on the frequency of the oscillations. This dependence contradicts the basic assumption about the time-invariance of the stability derivatives. The effect of frequency on the aerodynamic parameters is explained by a proposed formulation of the aerodynamic model equations with unsteady terms. In addition, this formulation separates the sums of derivatives, mentioned above, into two terms, one representing either the static or purely-rotary derivatives, and the other, the unsteady effects.

Attempts to analyze the wind tunnel oscillatory data with the inclusion of unsteady aerodynamic effects are reported in references 4 and 5. The purpose of this report is to develop a method for estimation of unknown parameters in mathematical models postulated for wind tunnel data from small amplitude oscillatory testing and demonstrate this method

in three examples. In the first example, the forced oscillatory data in pitch and roll of a triangular wing are analyzed. The second example uses the oscillatory data in pitch and roll of a model of the X-31 experimental aircraft. The third example deals with acceleration-in-sideslip data of a high incidence research model (HIRM). In this test, the model oscillates in sideslip at a specified angular velocity and amplitude (see reference 5). From the measured data, the aerodynamic derivatives corresponding to sideslip angle and its rate are calculated.

PARAMETER ESTIMATION

A parameter estimation algorithm is developed for the analysis of the normal force obtained from wind tunnel oscillatory data in pitch. Modification of this algorithm for oscillatory data in roll and yaw, and oscillatory data in heave and sideslip should be straightforward. As pointed out in reference 1, the equation for the normal force can be formulated as

$$C_N(t) = C_{N_\alpha}(\infty)\alpha(t) - \int_0^t F_\alpha(t-\tau)\frac{\mathrm{d}}{\mathrm{d}\tau}\alpha(\tau)\mathrm{d}\tau + \frac{\ell}{V}C_{N_q}(\infty)q(t) \qquad (1)$$

where

$C_{N_\alpha}(\infty)$ is the rate of change of C_N with α in steady flow evaluated at $q = 0$. This term corresponds to the stability derivative $\frac{\partial C_N}{\partial \alpha}$.

$C_{N_q}(\infty)$ is the rate of change of C_N with q in steady flow evaluated at α equal to its mean value during the oscillatory motion. This term corresponds to the stability derivative $\frac{\partial C_N}{\partial \frac{q\bar{c}}{2V}}$.

$F_\alpha(t)$ is the deficiency function which is defined as the difference between $C_{N_\alpha}(\infty)$and the indicial function $C_{N_\alpha}(t)$. Its analytical form, proposed in reference 1, is

$$F_\alpha(t) = ae^{-b_1 t}$$

which follows from the postulated indicial function

$$C_{N_\alpha}(t) = a\left(1 - e^{-b_1 t}\right) + c$$
$$= C_{N_\alpha}(\infty) - F_\alpha(t) \tag{2}$$

The steady-state form of equation (1) for harmonic changes in $\alpha(t)$ is given as

$$C_N(t) = \overline{C}_{N_\alpha} \alpha_A \sin(\omega t) + \frac{\ell}{V} \overline{C}_{N_q} \alpha_A \omega \cos(\omega t) \tag{3}$$

where

$\overline{C}_{N_\alpha}$ and $\overline{C}_{N_q}$ are the in-phase and out-of-phase components, respectively,
α_A is the amplitude of the oscillations,
ω is the angular frequency,
ℓ is the characteristic length, and
V is the airspeed.

As follows from the development in reference 1, the mathematical models for the components of $C_N(t)$ have the form

$$\overline{C}_{N_\alpha} = C_{N_\alpha}(\infty) - a\frac{\tau_1^2 k^2}{1 + \tau_1^2 k^2} \tag{4}$$

$$\overline{C}_{N_q} = C_{N_q}(\infty) - a\frac{\tau_1}{1 + \tau_1^2 k^2} \tag{5}$$

where τ_1 is related to the parameter b_1 as

$$\tau_1 = \frac{V}{b_1 \ell}$$

and k is the reduced frequency

$$k = \frac{\omega \ell}{V}$$

The second term on the right side of equations (4) and (5) represent the unsteady counterparts of $k^2 C_{N_{\dot{q}}}$ and $-C_{N_{\dot{\alpha}}}$, respectively. The parameter a accounts for the variation of the unsteady terms with the angle of attack.

From the experiment, the in-phase and out-of-phase components are usually obtained for different values of the angle of attack and reduced frequency while keeping the amplitude of the oscillations constant, that is

$$\left.\begin{matrix} \overline{C}_{N_\alpha}(\alpha_i, k_j) \\ \overline{C}_{N_q}(\alpha_i, k_j) \end{matrix}\right\} \begin{matrix} i = 1,2,\ldots,n \\ j = 1,2,\ldots,m \end{matrix}$$

Then equations (4) and (5) can be expressed as

$$\bar{u}_{ji} = u_i f(\alpha_i) - a_i z_{u_j} f(\alpha_i) \tag{6}$$

$$\bar{v}_{ji} = v_i - a_i z_{v_j} f(\alpha_i) \tag{7}$$

where

$$u_i = C_{N_\alpha}(\infty; \alpha_i), \qquad v_i = C_{N_q}(\infty; \alpha_i),$$

$$z_{u_j} = \frac{\tau_1^2 k_j^2}{1 + \tau_1^2 k_j^2}, \qquad z_{v_j} = \frac{\tau_1}{1 + \tau_1^2 k_j^2},$$

$$f(\alpha_i) = 1$$

The definition of z_{u_j} and z_{v_j} for oscillatory data in roll and yaw are identical to those for the data in pitch, but for the rolling oscillations, $f(\alpha) = \sin(\alpha)$ and for the yawing oscillations, $f(\alpha) = \pm\cos(\alpha)$ where the minus sign applies to the out-of-phase components.

In equations (6) and (7) there are, in general, $3n + 1$ unknown parameters: u_i, v_i, a_i, and τ_1. They can be estimated from experimental data $\bar{u}_{ji}$ and $\bar{v}_{ji}$ by minimizing the cost function

$$J = \sum_{j=1}^{m} \sum_{i=1}^{n} \left\{ \left[\bar{u}_{ji} - \left(u_i - a_i z_{u_j} \right) \right]^2 + \left[\bar{v}_{ji} - \left(v_i - a_i z_{v_j} \right) \right]^2 \right\} \tag{8}$$

This cost function is nonlinear in the parameter τ_1. To formulate a linear estimation problem, equations (6) and (7) are linearized about some nominal values of all unknown parameters. The linearized cost function takes the form

$$J = \sum_{j=1}^{m} \sum_{i=1}^{n} \left\{ \left[\bar{u}_{ji} - \left(u_i - a_i z_{u_j} \right)_0 - \Delta u_i + \left(z_{u_j} \right)_0 \Delta a_i + \left(a_i z^*_{u_j} \right)_0 \Delta \tau_1 \right]^2 \right.$$
$$\left. + \left[\bar{v}_{ji} - \left(v_i - a_i z_{v_j} \right)_0 - \Delta v_i + \left(z_{v_j} \right)_0 \Delta a_i + \left(a_i z^*_{v_j} \right)_0 \Delta \tau_1 \right]^2 \right\} \tag{9}$$

where

$$z^*_{u_j} = \frac{\partial}{\partial \tau_1} z_{u_j} = \frac{2\tau_1 k_j^2}{\left(1 + \tau_1^2 k_j^2\right)^2}$$

$$z^*_{v_j} = \frac{\partial}{\partial \tau_1} z_{v_j} = \frac{1 - \tau_1^2 k_j^2}{\left(1 + \tau_1^2 k_j^2\right)^2}$$

and the index 0 indicates nominal values.

Following the minimization of (9), the normal equations for unknown parameters can be formulated as

$$\Delta \hat{\boldsymbol{\theta}} = -\boldsymbol{M}^{-1} \left. \frac{\partial J}{\partial \boldsymbol{\theta}} \right|_{\boldsymbol{\theta}=\boldsymbol{\theta}_0} \tag{10}$$

where

$$\Delta \hat{\boldsymbol{\theta}} = \left[\Delta \hat{u}_i \; \Delta \hat{v}_i \; \Delta \hat{a}_i \; \Delta \hat{\tau}_1 \right]^{\mathrm{T}}$$

and $\boldsymbol{M}$ is the matrix formed by partial derivatives

$$\left. \frac{\partial \bar{u}_{ji}}{\partial \boldsymbol{\theta}} \right|_{\boldsymbol{\theta}=\boldsymbol{\theta}_0} \text{ and } \left. \frac{\partial \bar{v}_{ji}}{\partial \boldsymbol{\theta}} \right|_{\boldsymbol{\theta}=\boldsymbol{\theta}_0}$$

Parameter estimation using equation (10) is an iterative process where the estimates are obtained as

$$\hat{\boldsymbol{\theta}}_{r+1} = \hat{\boldsymbol{\theta}}_r + \Delta \hat{\boldsymbol{\theta}}_{r+1} \tag{11}$$

and where the index r indicates the r^{th} iteration. The parameter covariance matrix is estimated as

$$\mathrm{Cov}\left(\hat{\boldsymbol{\theta}}\right) = s^2 \boldsymbol{M}^{-1} \tag{12}$$

with the variance estimate

$$s^2 = \frac{J(\hat{\theta})}{2nm-(3n+1)} \tag{13}$$

For the estimation of all parameters in (6) and (7), the number of measured data must be equal to or greater than $3n+1$. This means that the experiment must be repeated for at least two different frequencies, that is $m \geq 2$. The estimation algorithm can be modified by the inclusion of $C_{N_\alpha}(\infty;\alpha_i)$ from static wind tunnel tests. Then the measured data $\bar{u}_{ji}$ will be replaced by $(\bar{u}_{ji}-u_i)$. The number of unknown parameters will be $2n+1$ and again, the condition $m \geq 2$ will have to be met. If, on the other hand, only the out-of-phase components $\bar{v}_{ji}$ are available, then the number of data points is nm, the number of unknown parameters is $2n+1$, and the condition for the number of frequencies is $m \geq 3$.

The model for the normal force of an aircraft performing one-degree-of-freedom harmonic oscillations in heave is formulated in Appendix A as

$$C_N(t) = \tilde{C}_{N_\alpha}\alpha_A \sin(\omega t) + \frac{\ell}{V}\tilde{C}_{N_{\dot{\alpha}}}\alpha_A \omega \cos(\omega t) \tag{14}$$

where

$$\tilde{C}_{N_\alpha} = C_{N_\alpha}(\infty) - a\frac{\tau_1^2 k^2}{1+\tau_1^2 k^2} \tag{15}$$

$$\tilde{C}_{N_{\dot{\alpha}}} = -a\frac{\tau_1}{1+\tau_1^2 k^2} \tag{16}$$

Following the previous development, equations (15) and (16) can be expressed in the form

$$\left.\begin{aligned} \tilde{u}_{ji} &= u_i - a_i z_{u_j} \\ \tilde{v}_{ji} &= -a_i z_{v_j} \end{aligned}\right\} \begin{aligned} i &= 1,2,\ldots,n \\ j &= 1,2,\ldots,m \end{aligned} \tag{17, 18}$$

The algorithm for estimation of unknown parameters u_i, a_i, and τ_1 can be obtained in the same way as for the parameters in equations (6) and (7).

The estimation algorithm using oscillatory data in roll and sideslip follows from the model developed in reference 1

$$\overline{C}_{l_\beta} = C_{l_\beta}(\infty)\sin(\alpha) - a\frac{\tau_1^2 k^2}{1+\tau_1^2 k^2}\sin(\alpha) \tag{19}$$

$$\overline{C}_{l_p} = C_{l_p}(\infty) - a\frac{\tau_1}{1+\tau_1^2 k^2}\sin(\alpha) \tag{20}$$

and from the model developed in Appendix A

$$\tilde{C}_{l_\beta} = C_{l_\beta}(\infty) - a\frac{\tau_1^2 k^2}{1+\tau_1^2 k^2} \tag{21}$$

$$\tilde{C}_{l_{\dot\beta}} = -a\frac{\tau_1}{1+\tau_1^2 k^2} \tag{22}$$

Similar to the expressions for the oscillatory data in pitch, the second term on the right side of equations (19) and (20) are the unsteady counterparts of $k^2 C_{l_{\dot p}}$ and $-C_{l_{\dot\beta}}\sin(\alpha)$, respectively.

EXAMPLES

The estimation algorithm developed is applied to measured oscillatory data in three examples. In the first example, parameters of a triangular wing subjected to forced oscillations in pitch and roll are estimated. The second example again presents the analysis of oscillatory data in pitch and roll this time, however, measured for a 19-percent-scale model of the X-31 experimental aircraft. Finally, in the third example, parameter estimates are obtained from data due to acceleration in sideslip of the High Incidence Research Model 2 (HIRM 2). A sketch of the last two models is given in figure 1 together with the numerical values of their basic geometric characteristics.

Forced Oscillations of 70° Triangular Wing

The oscillatory data of a triangular wing were obtained from reference 5. The model had the span, b = 0.90 m, mean aerodynamic chord, $\bar{c}$ = 0.824 m, and sweep angle of the leading edge of 70°. The model was tested in pitch and roll at two center-of-gravity (axis of rotation)

locations, $0.25\bar{c}$ and $0.50\bar{c}$, and at angles of attack between -4° and 57°. The frequencies varied between 0.5 and 2.5 Hz and the amplitudes of the oscillations were 3° and 5°. The experiment was conducted at the speed of 45 m/sec corresponding to a mean-chord Reynolds number of about $2\text{x}10^6$. Reference 5 contains only a limited number of test data: the in-phase and out-of-phase components of the normal force and the out-of-phase components of the pitching and rolling moment. For parameter estimation, the data with the amplitude of 3° and c.g. location of $0.50\bar{c}$ were chosen. The following three sets of data were used in the analysis:

1. $\overline{C}_{N_\alpha}(\alpha_i, k_j)$ and $\overline{C}_{N_q}(\alpha_i, k_j)$ at three frequencies and eight values of the angle of attack between 27° and 56 °,
2. $\overline{C}_{m_q}(\alpha_i, k_j)$ at five frequencies and the same values of angle of attack as in the preceding set,
3. $\overline{C}_{l_p}(\alpha_i, k_j)$ at five frequencies and fourteen values of the angle of attack between 5° and 57°.

The measured data are plotted against the angle of attack with the reduced frequency as a parameter in figures 2, 4, 5, 7, and 8.

The parameter estimation algorithm for data set $\overline{C}_{N_\alpha}, \overline{C}_{N_q}$ was based on model equations (4) and (5); for data of $\overline{C}_{m_q}$, on equation (5); and for data of $\overline{C}_{l_p}$, on equation (20). The estimates of the nondimensional time delay, τ_1, and computed values of parameters $b_1 = \dfrac{V}{\ell\tau_1}$ and $T_1 = \dfrac{1}{b_1}$ for all data sets are given in table I. The values of τ_1 are similar for the normal-force and pitching-moment indicial functions, and only slightly higher for the rolling-moment indicial function. The increased number of data points due to increased number of frequencies from 3 to 5 improved substantially the accuracy of the estimated parameter τ_1.

Estimates of parameter a in the indicial function and derivatives $C_{N_\alpha}(\infty)$, $C_{N_q}(\infty)$, $C_{m_q}(\infty)$, and $C_{l_p}(\infty)$ are plotted in figures 3, 6, and 9. The minimum and maximum values of their standard errors are presented in table II. All the estimates mentioned are obtained from data at three frequencies. Contrary to the estimates of τ_1, increasing the number of frequencies from 3 to 5 had only a small effect on the estimates of the remaining parameters and their covariances.

In figure 3, the estimates of $C_{N_\alpha}(\infty)$ are compared with the results of a static wind tunnel test. The agreement between estimates and measured data is very good. This agreement can be interpreted as a confidence in the postulated model for $\overline{C}_{N_\alpha}$ and $\overline{C}_{N_q}$. The model was further verified by a comparison of the measured and estimated values of the oscillatory data and by checking the model prediction capabilities. In figures 2, 4, and 7 the measured data are plotted together with those estimated from model equations after substituting the parameter estimates. The agreement between measurement and estimation is very good. In figure 5, the measured values of $\overline{C}_{m_q}$ are compared with those predicted at two frequencies not used in the parameter estimation. As in the previous cases, the predictions agree very well with the measured data. Similar agreement can be seen in figure 8 where the measured and predicted values of $\overline{C}_{l_p}$ are shown.

If the measured data are obtained only for a limited number of frequencies, good agreement between measured and estimated points in itself cannot be considered as a verification of the model adequacy. As follows from equations (4) and (5), at each selected angle of attack there are four parameters which are to be estimated from $2m$ data points of the in-phase and out-of-phase components. If $m = 2$, only the constraints a.) τ_1 has the same value for all α_i and b.) a_i has the same values for $\overline{C}_{N_\alpha}$ and $\overline{C}_{N_q}$ prevented complete agreement between measured and estimated data. Accurate parameter estimation and model verification would, therefore, require measurement of the in-phase and out-of-phase components at an increased number of frequencies (four or more for estimation, one for verification) and static wind tunnel testing for obtaining aerodynamic derivatives in the model equations.

Forced Oscillations of X-31 Model

The forced-oscillation test on the model of the X-31 aircraft were conducted at the 30-by-60 foot wind tunnel at NASA Langley Research Center. During the test, the dynamic pressure at the tunnel was 10 lb/ft^2 (478.8 Pa) and the Reynolds number referred to $\bar{c}$ was 1.37x10^6. From wind tunnel results, three sets of data were selected for parameter estimation:

1. $\overline{C}_{N_\alpha}$ and $\overline{C}_{N_q}$ at two frequencies of 0.8 and 1.2 Hz and $0° \leq \alpha \leq 87.5°$,
2. $\overline{C}_{m_\alpha}$ and $\overline{C}_{m_q}$ at the same frequencies and angles of attack,
3. $\overline{C}_{l_\beta}$ and $\overline{C}_{l_p}$ at two frequencies of 0.4 and 0.6 Hz and $25° \leq \alpha \leq 50°$.

The amplitude of oscillations was 5°. The positions of the control surfaces were as follows: the trailing edge, 0°; leading edge, 40° (inboard) and 32° (outboard); and canard, -40°. Some of the measured data are available in reference 7.

Similar to the previous example, model equations (4),(5),(19), and (20) were used. The measured and estimated values of $\overline{C}_{N_\alpha}$ and $\overline{C}_{N_q}$ are shown in figure 10. The estimated points are almost identical or close to the measured data. This closeness is the result of the small number of data points for a given angle of attack, as pointed out in the previous example. The estimated parameters τ_1 and computed parameters b_1 and T_1 are given in table II together with the same parameters estimated from the remaining two sets of data. The parameters $C_{N_\alpha}(\infty)$, $C_{N_q}(\infty)$, and α are plotted in figure 11. Substantial differences in the derivative $C_{N_\alpha}(\infty)$ estimated from the oscillatory and static measurement and large scatter in the estimates of $C_{N_q}(\infty)$ around the fitted curve are apparent.

Estimated parameters from data sets $\overline{C}_{m_\alpha}$, $\overline{C}_{m_q}$ and $\overline{C}_{l_\beta}$, and $\overline{C}_{l_p}$ are presented in figures 12 to 15. These estimates have problems similar to those mentioned before. In addition, the review of $\overline{C}_{l_p}$ at various frequencies, amplitudes, and configurations presented in figure 16 leads to the conclusion that the estimates of $C_{l_p}(\infty)$ in figure 15, for angles of attack between 25° and 35°, have values far from those expected. Low parameter accuracy and differences in derivatives $C_{N_\alpha}(\infty)$, $C_{m_\alpha}(\infty)$, and $C_{l_\beta}(\infty)$ from oscillatory and static measurements could be caused by a small number of data points, measured data accuracy, and by modeling errors in postulated models used in parameter estimation. For obtaining more accurate results, it would be necessary to have the oscillatory data (both in-phase and out-of-phase) at more frequencies and more values of the angle of attack within the selected range.

In-sideslip Oscillations of HIRM 2

A description of the HIRM 2, testing method and conditions of the test, and some of the results are given in reference 5. The experiment was conducted in the 13-by-19 foot low speed wind tunnel at the Defense Research Agency (formerly Royal Aircraft Establishment) in Bedford, United Kingdom. The wind speed was approximately 30 m/sec which corresponds to a Reynolds number of about 1.1×10^6. For parameter estimation, two sets of data were selected:

1. $\tilde{C}_{l_\beta}$ and $\tilde{C}_{l_{\dot{\beta}}}$ at three frequencies of 2, 3, and 4 Hz and sixteen angles of attack between 0° and 42°, canard off,
2. $\tilde{C}_{l_\beta}$ and $\tilde{C}_{l_{\dot{\beta}}}$ at the same test conditions, but with the canard on at 0° setting.

The model for the measured data is represented by equations (21) and (22) with three unknown parameters $C_{l_\beta}(\infty)$, a, and τ_1. The estimated and computed parameters τ_1, b_1, and T_1 are summarized in table IV. These parameters have the same values for both configurations. The time constant T_1 is about one-third of that in the two previous examples. This means that the unsteady effect in sideslip oscillations of the HIRM 2 is less pronounced that in the oscillatory motions of the triangular wing and the X-31 model. The estimated values of $\tilde{C}_{l_\beta}$ and $\tilde{C}_{l_{\dot{\beta}}}$ presented in figures 17, 18, 20, and 21 are mostly close to the measured data which might be considered as the first indication of an adequate model for the given data. The remaining two parameters are plotted in figure 19 and 22. Rather large differences exist between estimates of $C_{l_\beta}(\infty)$ from oscillatory and static wind tunnel data obtained from reference 8. The reason for this disagreement was not found. No further model verification was possible due to the limited amount of measured data points. Plots of the parameter a indicate that, for the angles of attack between 0° and 25°, the effect of unsteady aerodynamics is very small. Therefore, for better understanding of the unsteady phenomenon and its modeling, it would be necessary to increase the number of data points by increasing the number of frequencies and selected values of angle of attack within the range from 25° to 50°.

CONCLUDING REMARKS

Using nonlinear least squares, an estimation algorithm for aircraft aerodynamic parameter estimation from wind tunnel oscillatory data was developed. Models of an aircraft in one-degree-of-freedom, small-amplitude, harmonic motion included unsteady terms in the form of indicial functions. In formulating analytical form of indicial functions for this type of data analysis two conflicting requirements must be addressed: parameter estimation requires a simple model with a small number of parameters in order to insure their reliability; on the other hand, a simple model will not completely explain the rich and complex phenomena at various scales associated with unsteady and separated flow during oscillatory or transient motion. The indicial functions were postulated as simple exponential forms where the unknown parameters included aerodynamic derivative, the exponent and multiplication term. It is important to realize that the model proposed in this work should be used in the analysis of experimental oscillatory data where the effect of frequency at a given nominal angle of attack and Reynolds number is considered. For different applications the proposed form of indicial functions should be carefully considered.

The estimation procedure was applied in three examples to the oscillatory data in pitch and roll of a 70° triangular wing and an X-31 model, and to in-sideslip oscillatory data of the High Incidence Research Model 2 (HIRM 2). From postulated models and examples, the following conclusions can be drawn:

1. An aerodynamic model with a simple form of the indicial function included can "explain" unsteady effects observed in small-amplitude, oscillatory wind tunnel data;
2. the accuracy of estimated parameters and model verification could be strongly influenced by the number of measured data points and their accuracy;
3. future wind tunnel experiments intended for parameter estimation should include oscillatory data (both in-phase and out-of-phase components) at a large number of frequencies, five or more, and at an

increased number of angles of attack in the region where unsteady effects can be expected;

4. the wind tunnel experiment should also include measurements for obtaining static stability derivatives and purely-rotary derivatives for a comparison with their estimates from oscillatory data.

REFERENCES

1. Klein, Vladislav and Noderer, Keith D.: Modeling of Aircraft Unsteady Aerodynamic Characteristics. Part I - Postulated Models, NASA TM 109120, 1994.
2. Grafton, Sue B. and Libbey, Charles E.: Dynamic Stability Derivatives of a Twin-Jet Fighter Model for Angles of Attack from -10° to 110°. NASA TN D-6091, 1971.
3. Goman, M. G.; Stolyarov, G. I.; Tyrtyshnikov, S. L.; Usoltsev, S. P.; and Khrabrov, A. N.: Mathematical Description of Aircraft Longitudinal Aerodynamic Characteristics at High Angles of Attack Accounting for Dynamic Effects of Separated Flow. TsAGI Preprint No. 9, 1990 (in Russian).
4. Goman, M. and Khrabrov, A.: State-Space Representation of Aerodynamic Characteristics of an Aircraft at High Angles of Attack. *Journal of Aircraft*, Vol. 31, No. 5, Sept. - Oct. 1994, pp. 1109 - 1115.
5. O' Leary, C. O.; Weir, B.; and Walker, J. M.: Measurement of Derivatives due to Acceleration in Heave and Sideslip. In : Manoeuvring Aerodynamics, AGARD-CP-497, 1991, pp. 9-1 to 9-11.
6. Zhuk, A. N.; Ioselevitch, A. S.; Stolarov, G. I. and Tabatchnikov, V. G.: Experimental Investigation of Damping in Roll and Pitch of a Triangular Wing with Aspect Ratio 1.5 at High Angles of Attack. Proceedings of TsAGI, Issue 2290, 1985 (in Russian).
7. Villeta, Jose R.: Lateral-Directional Static and Dynamic Stability Analysis at High Angles of Attack for the X-31 Configuration. M.S. Thesis, The George Washington University, Washington, D.C., 1992.
8. O' Leary, C. O. and Weir, B.: The Effects of Foreplane on the Static and Dynamic Characteristics of a Combat Aircraft Model. Defense Research Agency, United Kingdom, TM Aero 2169, 1989.

APPENDIX A

HARMONIC OSCILLATORY MOTION IN HEAVE AND SIDESLIP

Using equations (1) and (2), the expression for the normal force of an aircraft performing a one-degree-of-freedom (o.d.f.) oscillatory motion in heave has the form

$$C_N(t) = C_{N_\alpha}(\infty)\alpha(t) - a\int_0^t e^{-b_1(t-\tau)}\frac{\mathrm{d}}{\mathrm{d}\tau}\alpha(\tau)\mathrm{d}\tau \tag{A.1}$$

Applying the Laplace transform to (A.1), the expression for the normal-force coefficient is obtained as

$$C_N(s) = \left(C_{N_\alpha} - \frac{as}{s+b_1}\right)\alpha(s) \tag{A.2}$$

where, for simplicity, $C_{N_\alpha} \equiv C_{N_\alpha}(\infty)$.

Using a complex expression for harmonic changes in $\alpha(t)$, that is

$$\alpha(t) = \alpha_A e^{i\omega t} = \alpha_A\left[\cos(\omega t) + i\sin(\omega t)\right]$$

and replacing s by $i\omega$, the steady-state solution to equation (A.2) is

$$C_N(t) = \left(C_{N_\alpha} - a\frac{\omega^2}{b_1^2+\omega^2}\right)\alpha_A\sin(\omega t) - a\frac{b_1}{b_1^2+\omega^2}\alpha_A\omega\cos(\omega t) \tag{A.3}$$

The introduction of reduced frequency $k = \frac{\omega\ell}{V}$ and nondimensional time constant $\tau_1 = \frac{V}{b_1\ell}$ yields

$$C_N(t) = \tilde{C}_{N_\alpha}\alpha_A\sin(\omega t) + \tilde{C}_{N_{\dot\alpha}}\alpha_A k\cos(\omega t) \tag{A.4}$$

where

$$\tilde{C}_{N_\alpha} = C_{N_\alpha}(\infty) - a\frac{\tau_1^2k^2}{1+\tau_1^2k^2} \tag{A.5}$$

$$\tilde{C}_{N_{\dot\alpha}} = -a\frac{\tau_1}{1+\tau_1^2k^2} \tag{A.6}$$

Similar expressions can be obtained for the pitching moment coefficient, $C_m(t)$.

Based on the analogy with the preceding case, the rolling-moment coefficient of an aircraft performing a o.d.f. oscillatory motion in sideslip has the form

$$C_l(t) = \tilde{C}_{l_\beta}\beta_A \sin(\omega t) + \tilde{C}_{l_{\dot{\beta}}}\beta_A k \cos(\omega t) \tag{A.7}$$

where

$$\tilde{C}_{l_\beta} = C_{l_\beta}(\infty) - a\frac{\tau_1^2 k^2}{1+\tau_1^2 k^2} \tag{A.8}$$

$$\tilde{C}_{l_{\dot{\beta}}} = -a\frac{\tau_1}{1+\tau_1^2 k^2} \tag{A.9}$$

The expressions for the side-force and yawing-moment coefficient are identical to those in equations (A.7) through (A.9).

Table I. Estimated and computed parameters. 70° triangular wing.

Measured data	Number of frequencies	Parameter		
		τ_1	b_1, sec^{-1}	T_1, sec
$\overline{C}_{N_\alpha}, \overline{C}_{N_q}$	3	$24.3 \pm 0.29^*$	4.5	0.22
$\overline{C}_{m_q}$	3	$30. \pm 6.7$	3.6	0.28
	5	$29. \pm 3.0$	3.8	0.27
$\overline{C}_{l_p}$	3	$40. \pm 12.$	2.5	0.40
	5	$31. \pm 2.3$	3.2	0.31

* the second value indicates the standard error

Table II. Minimum and maximum values of standard errors of estimated parameter. 70° triangular wing.

Measured data	Standard error			
	$s(\hat{a})$		$s\left(\hat{C}_{A_a}(\infty)\right)^*$	
	min	max	min	max
$\overline{C}_{N_\alpha}$	0.040	0.050	0.25	0.42
$\overline{C}_{N_q}$			0.40	0.46
$\overline{C}_{m_q}$	0.036	0.091	0.37	0.95
$\overline{C}_{l_p}$	0.008	0.036	0.059	0.20

* for index $A_a = N_\alpha, N_q, m_q,$ or l_p

Table III. Estimated and computed parameters. X-31 model.

Measured data	Parameter		
	τ_1	b_1, sec^{-1}	T_1, sec
$\overline{C}_{N_\alpha}, \overline{C}_{N_q}$	$23.4 \pm 0.33^*$	3.3	0.30
$\overline{C}_{m_\alpha}, \overline{C}_{m_q}$	$13. \pm 1.4$	6.0	0.17
$\overline{C}_{l_\beta}, \overline{C}_{l_p}$	$10. \pm 3.0$	4.2	0.24

* the second value indicates the standard error

Table IV. Estimated and computed parameters. HIRM 2.

Measured data	Parameter		
	τ_1	b_1, sec^{-1}	T_1, sec
$\tilde{C}_{l_\beta}, \tilde{C}_{l_{\dot{\beta}}}$ canard off	$4.6 \pm 0.38^*$	11.8	0.085
$\tilde{C}_{l_\beta}, \tilde{C}_{l_{\dot{\beta}}}$ canard on	4.5 ± 0.41	12.0	0.083

* the second value indicates the standard error

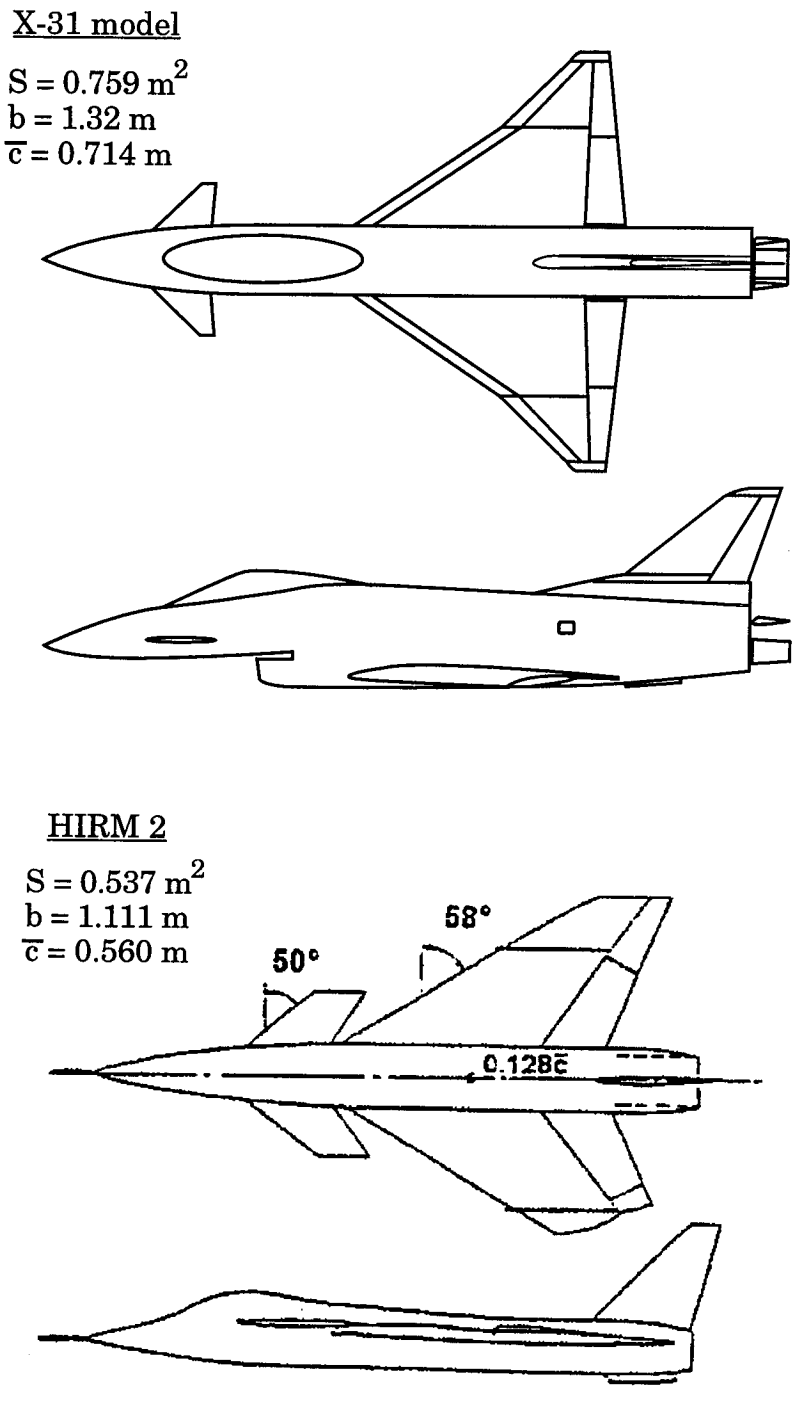

Figure 1. Two-view sketch of X-31 model and HIRM 2.

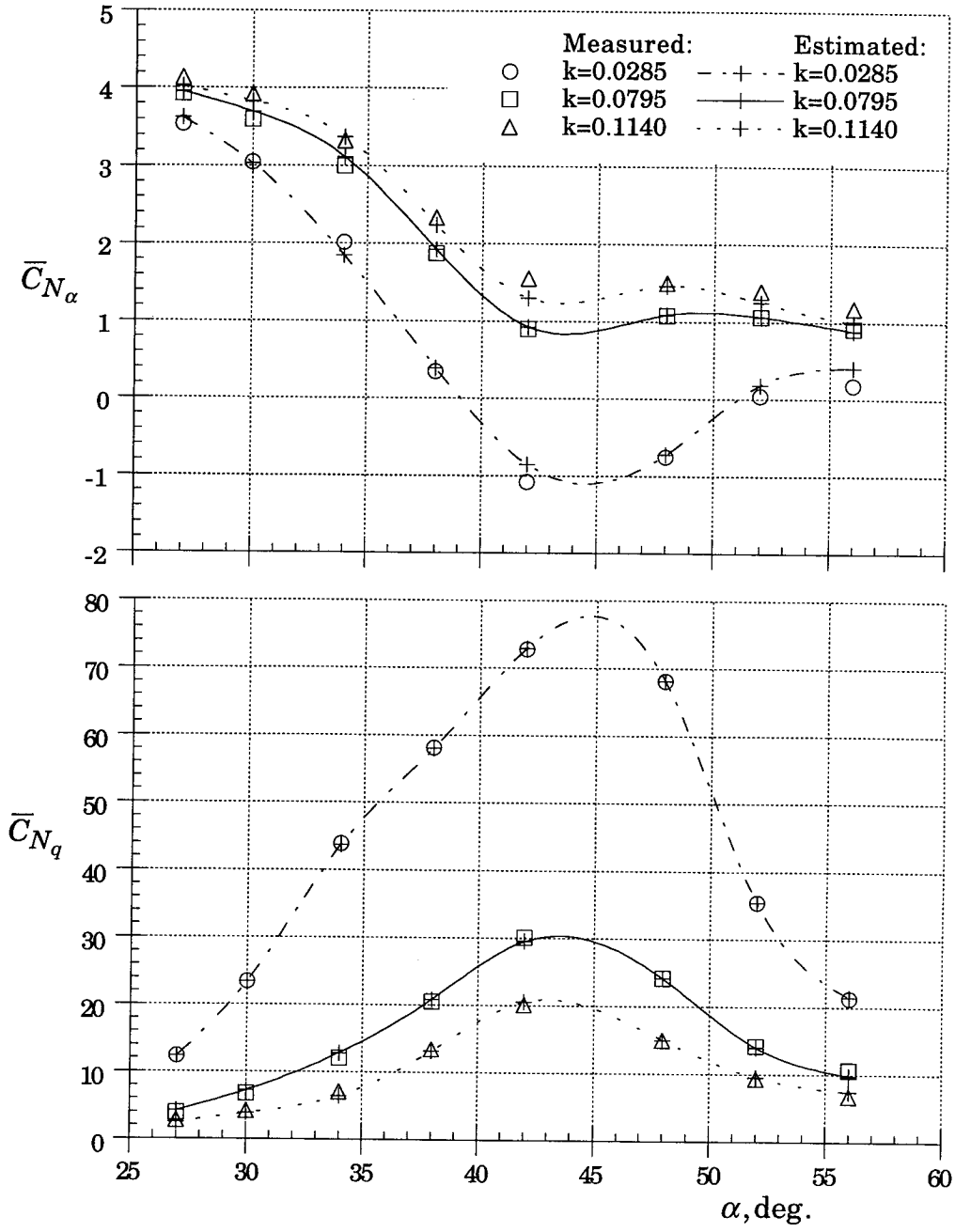

Figure 2. Measured and estimated in-phase and out-of-phase components of normal force. 70° triangular wing.

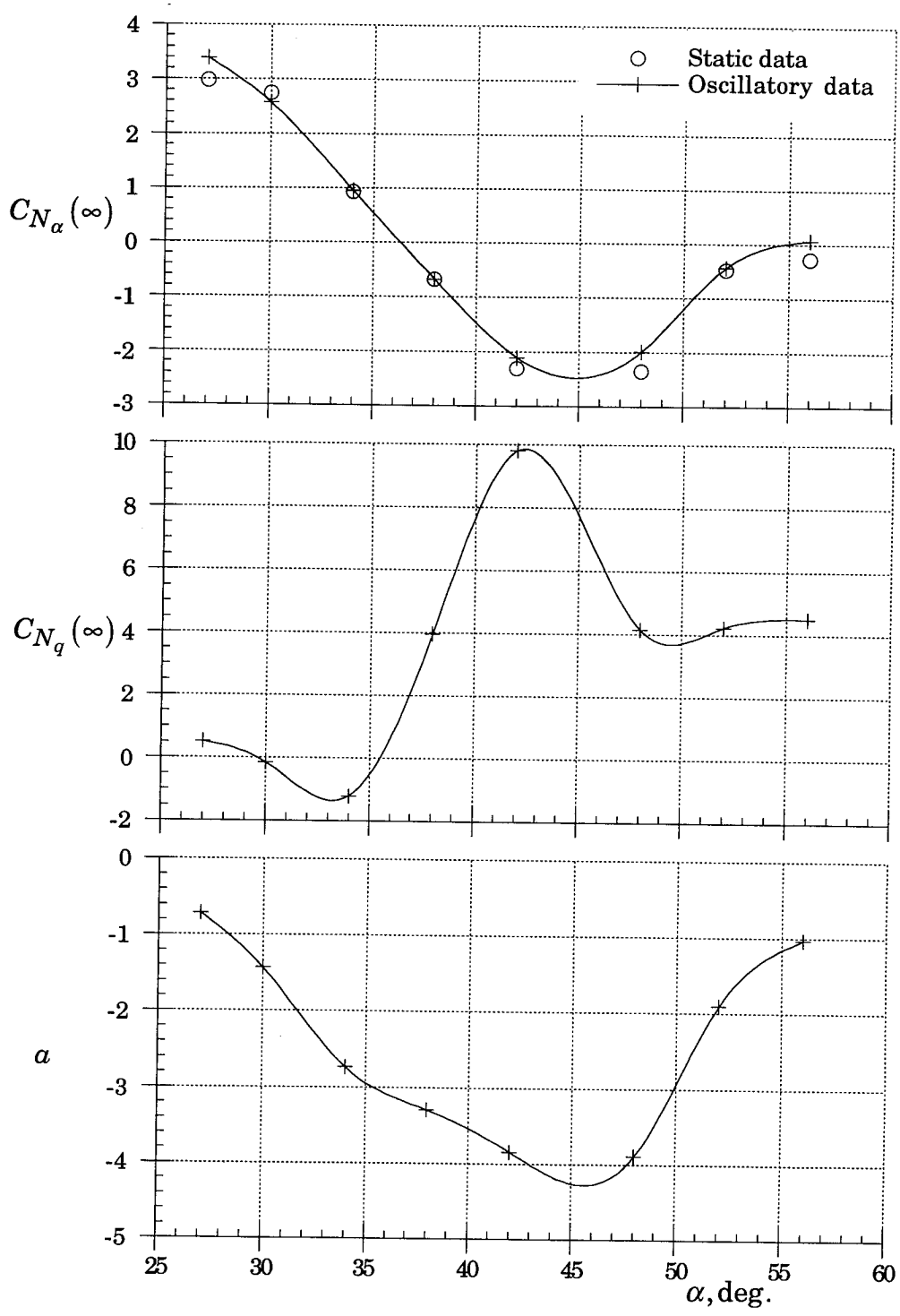

Figure 3. Estimated parameters of normal-force components. 70° triangular wing.

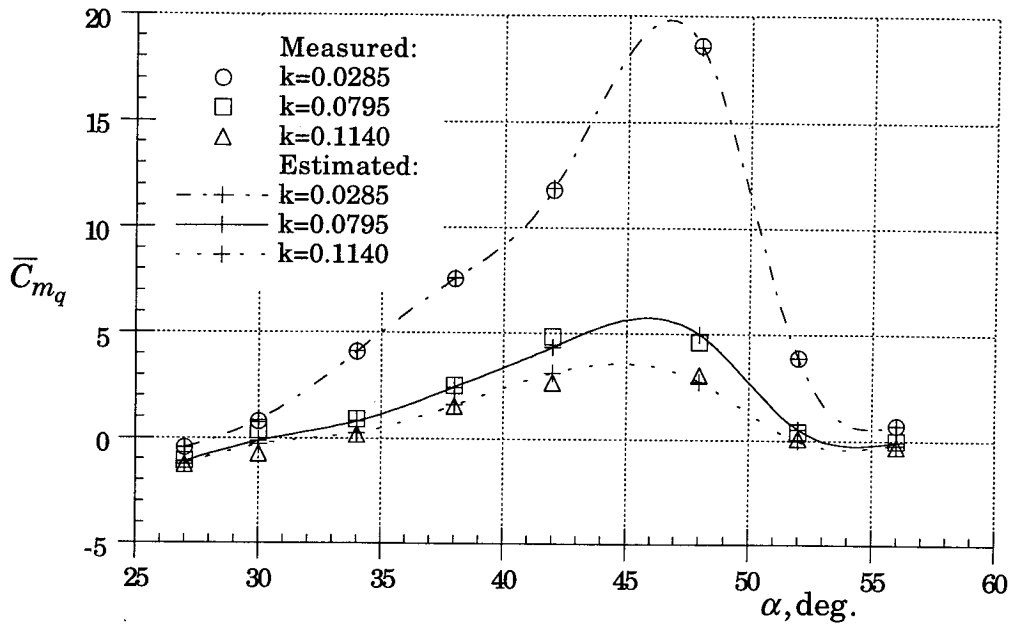

Figure 4. Measured and estimated out-of-phase components in pitching moment. 70° triangular wing.

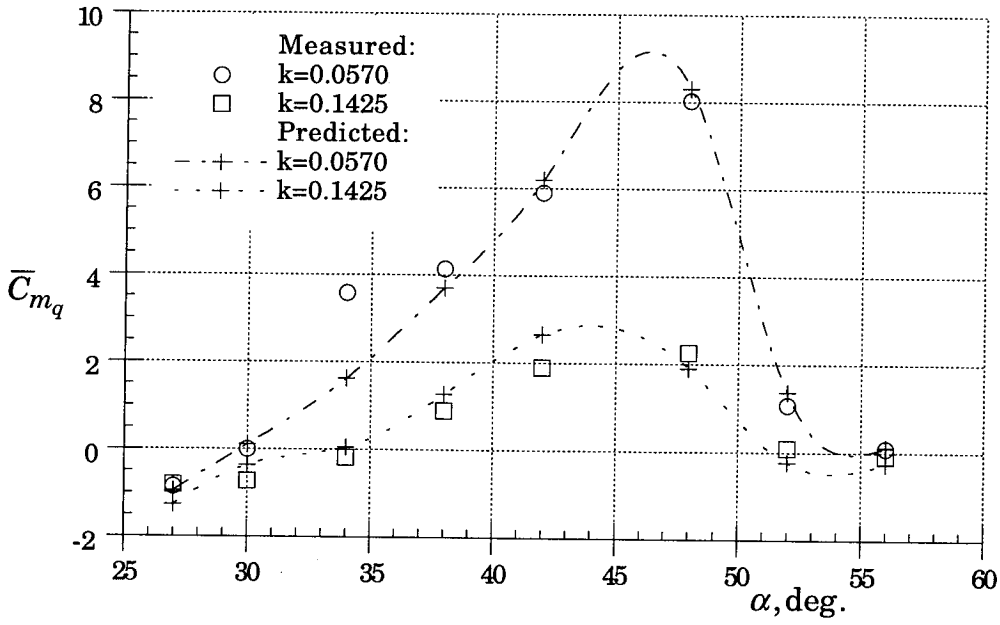

Figure 5. Measured and predicted out-of-phase components of pitching moment. 70° triangular wing.

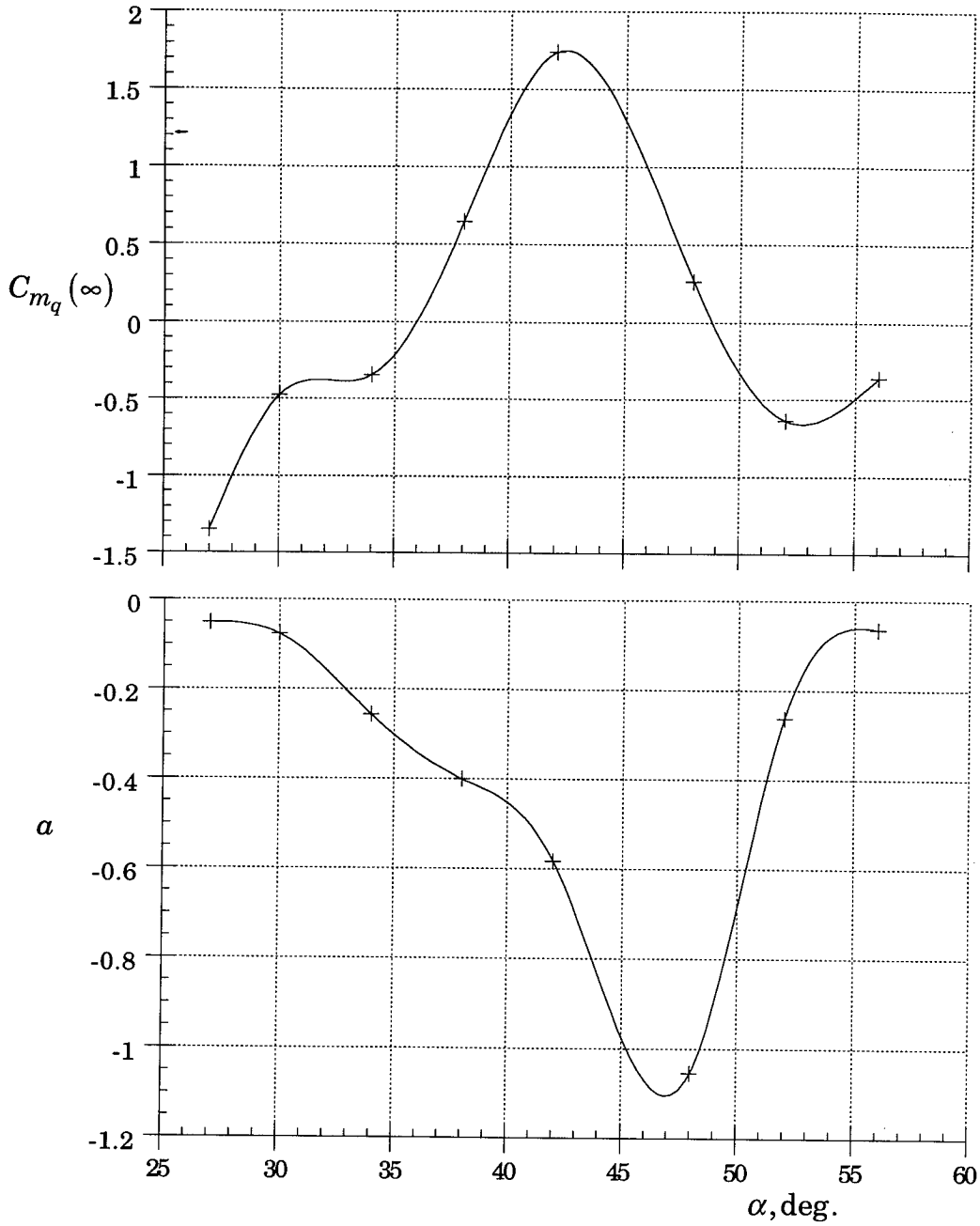

Figure 6. Estimated parameters of pitching-moment component. 70° triangular wing.

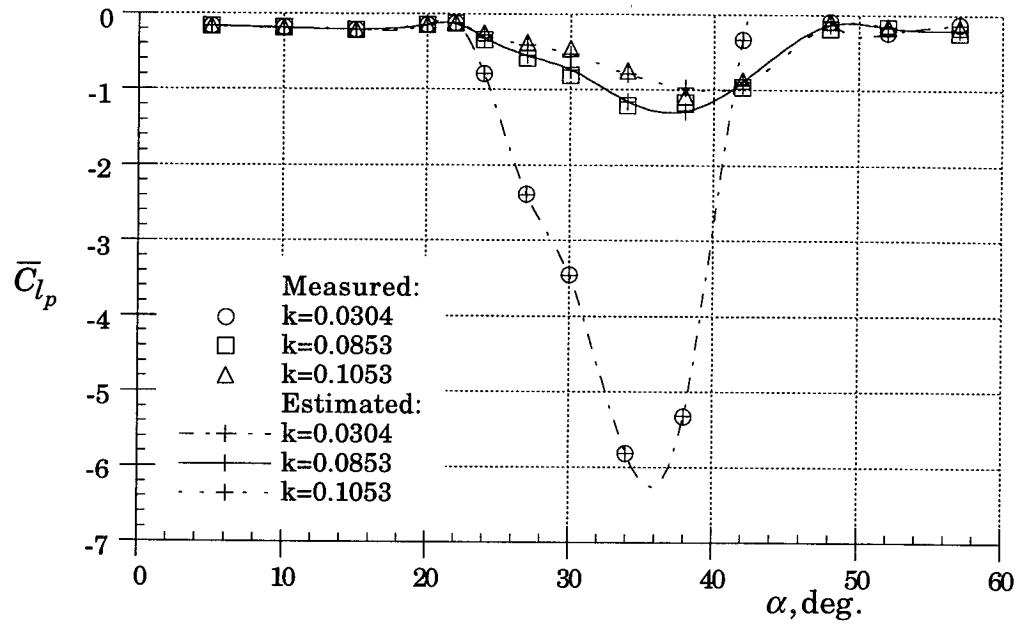

Figure 7. Measured and estimated out-of-phase components of rolling moment. 70° triangular wing.

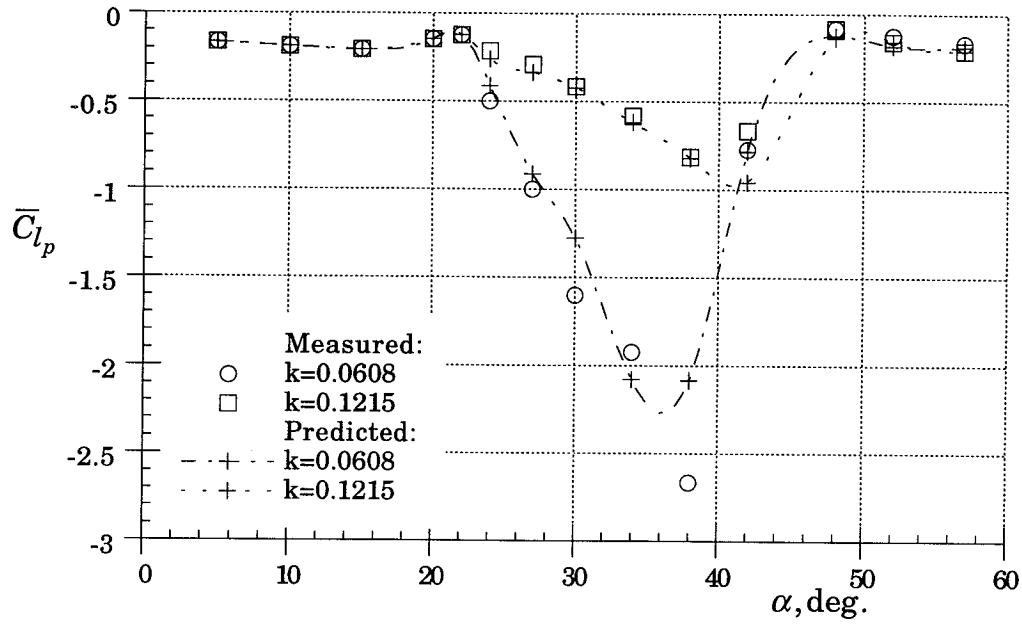

Figure 8. Measured and predicted out-of-phase components of rolling moment. 70° triangular wing.

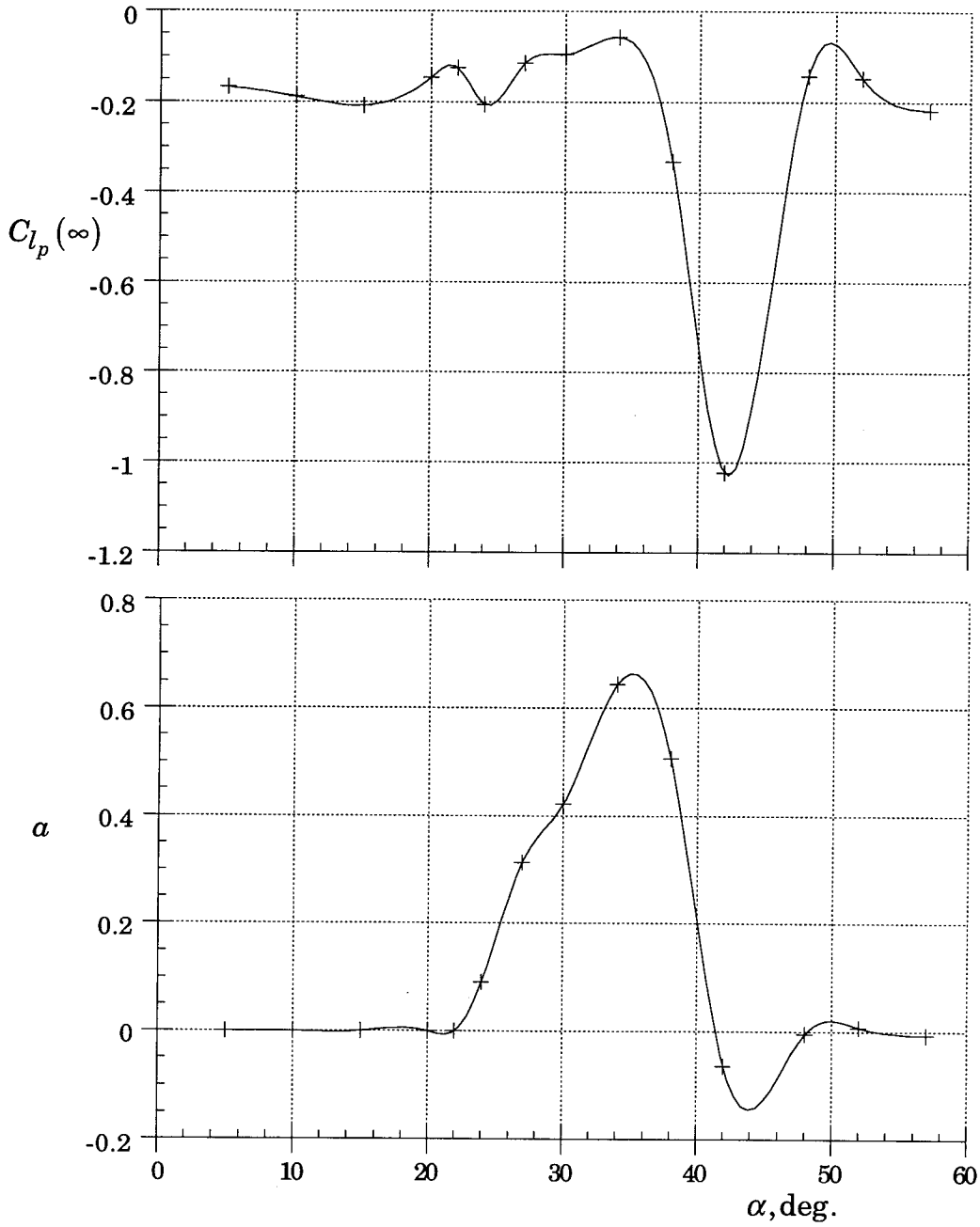

Figure 9. Estimated parameters of rolling-moment component. 70° triangular wing.

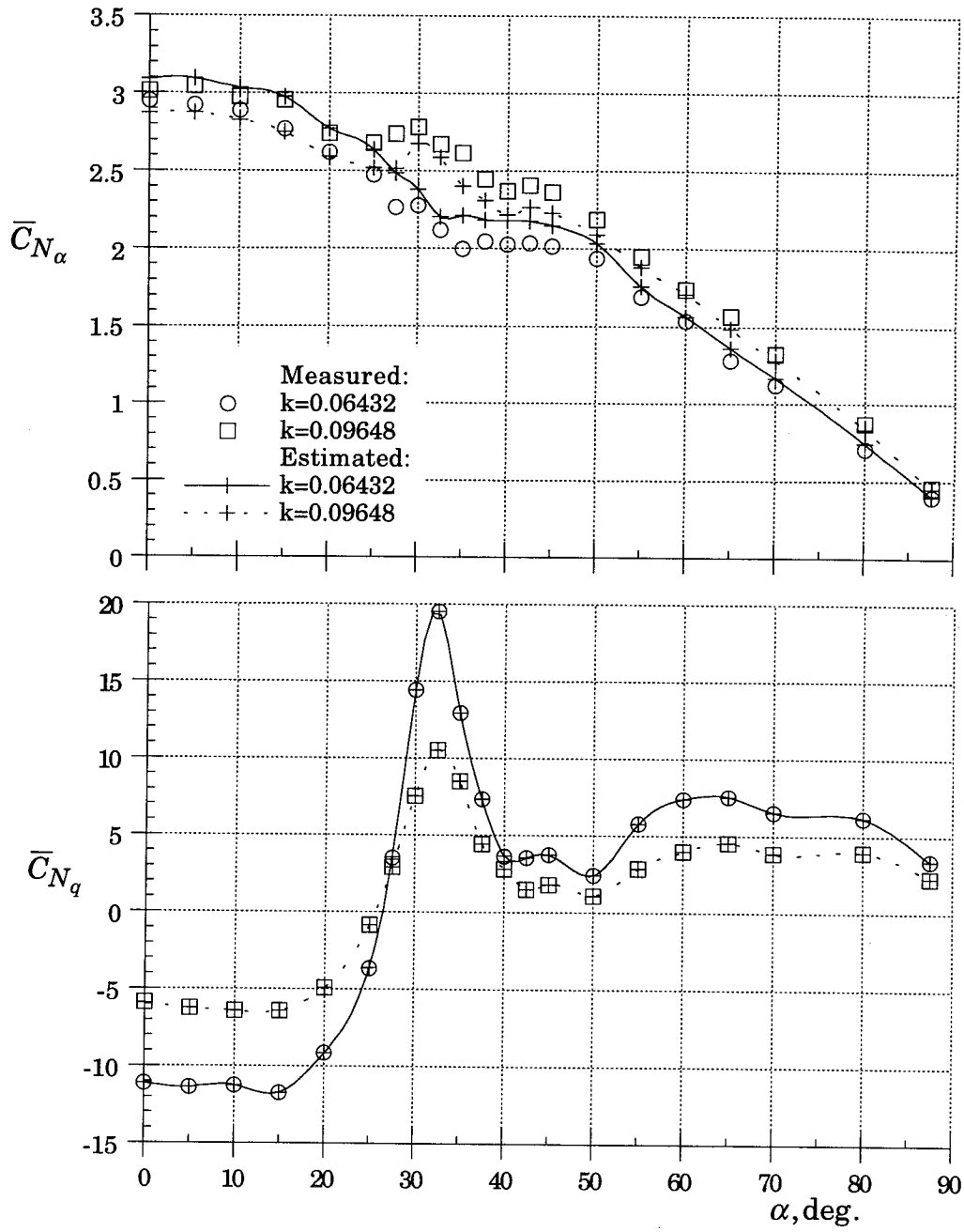

Figure 10. Measured and estimated in-phase and out-of-phase components of normal force. X-31 model.

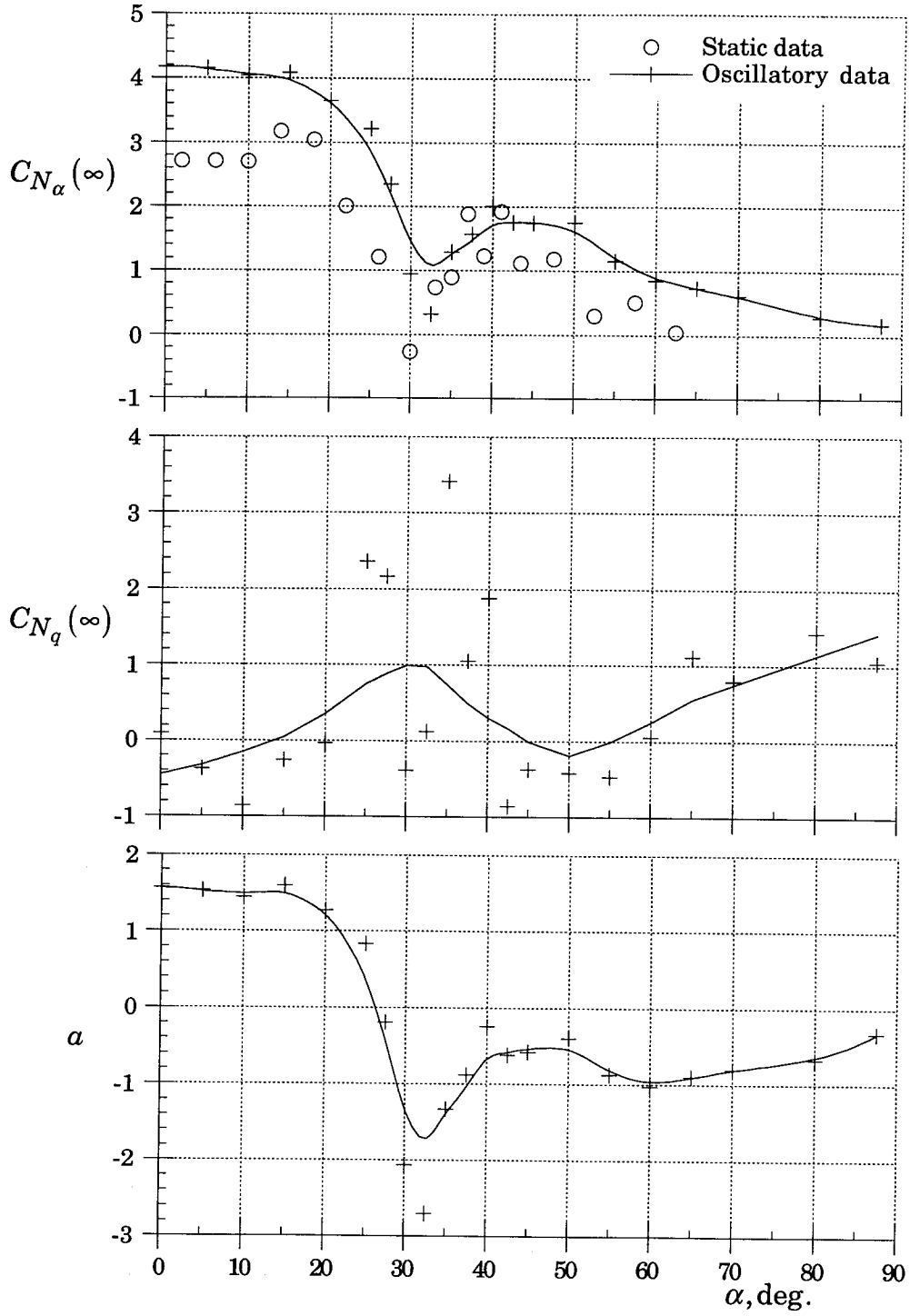

Figure 11. Estimated parameters of normal-force components. X-31 model.

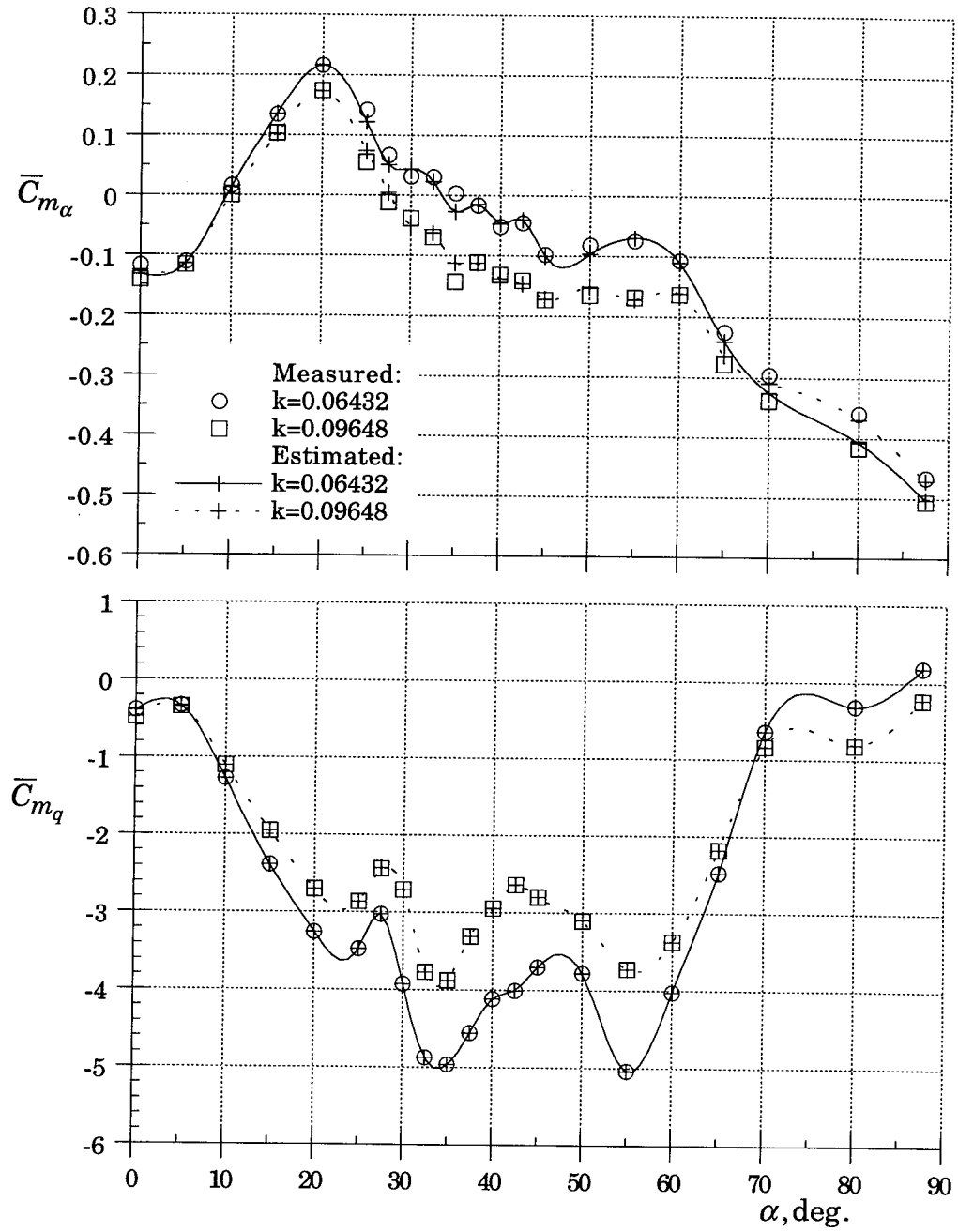

Figure 12. Measured and estimated in-phase and out-of-phase components of pitching moment. X-31 model.

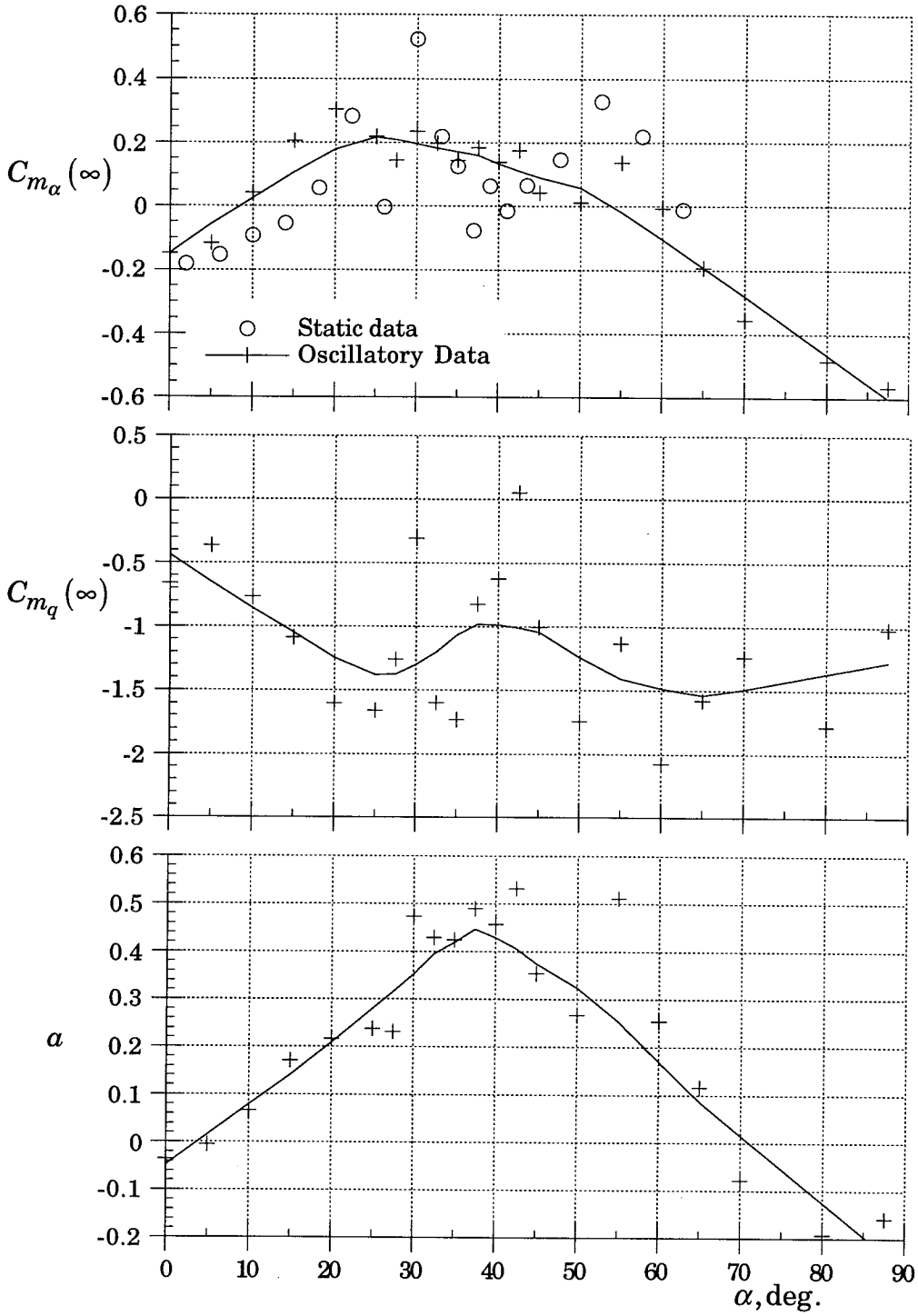

Figure 13. Estimated parameters of pitching-moment components. X-31 model.

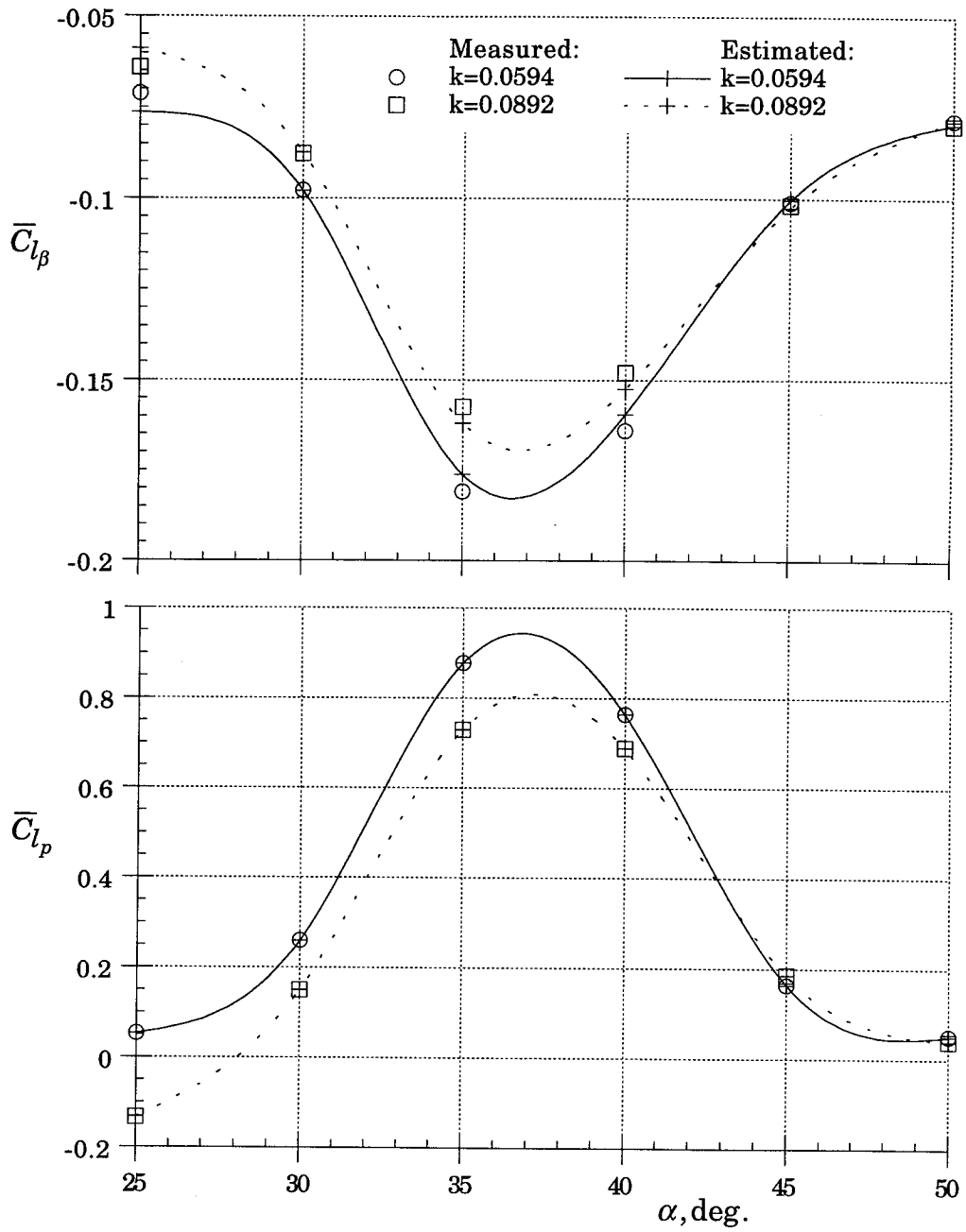

Figure 14. Measured and estimated in-phase and out-of-phase components of pitching moment. X-31 model.

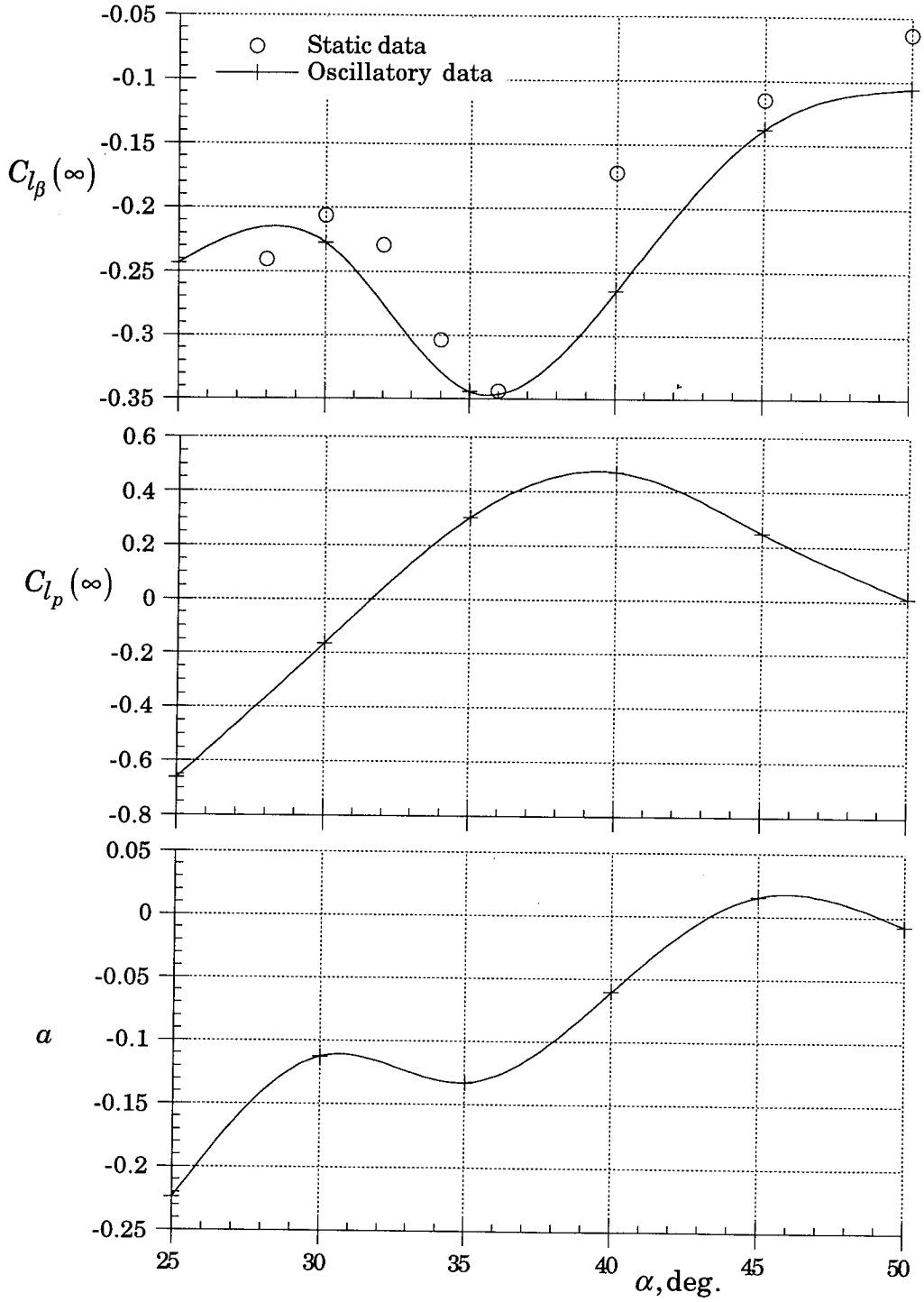

Figure 15. Estimated parameters of rolling-moment components. X-31 model.

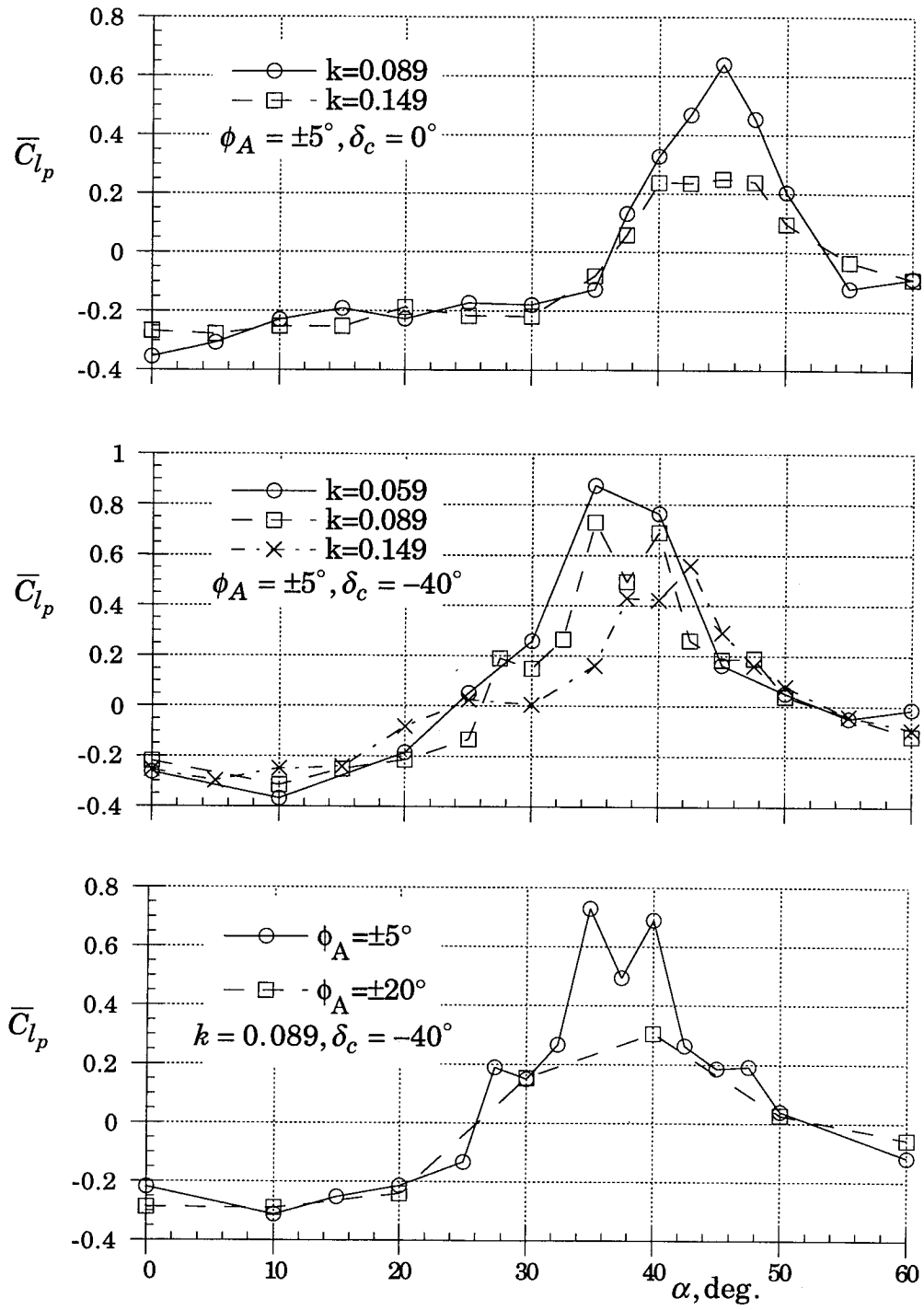

Figure 16. Effect of canard setting, frequency, and amplitude of oscillations on out-of-phase component of rolling moment. X-31 model

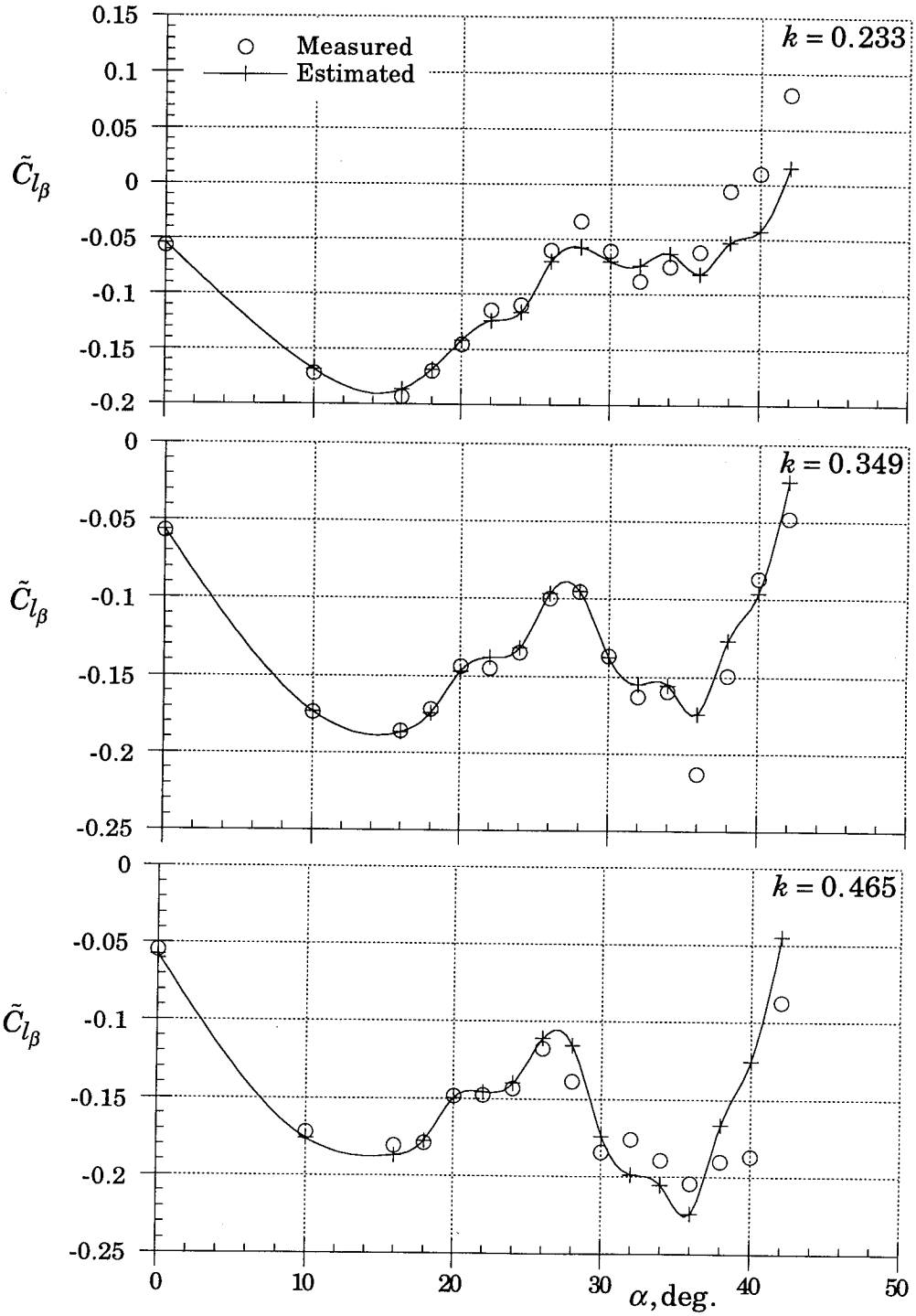

Figure 17. Measured and estimated in-phase components of rolling moment. In-sideslip oscillations of HIRM 2, canard off.

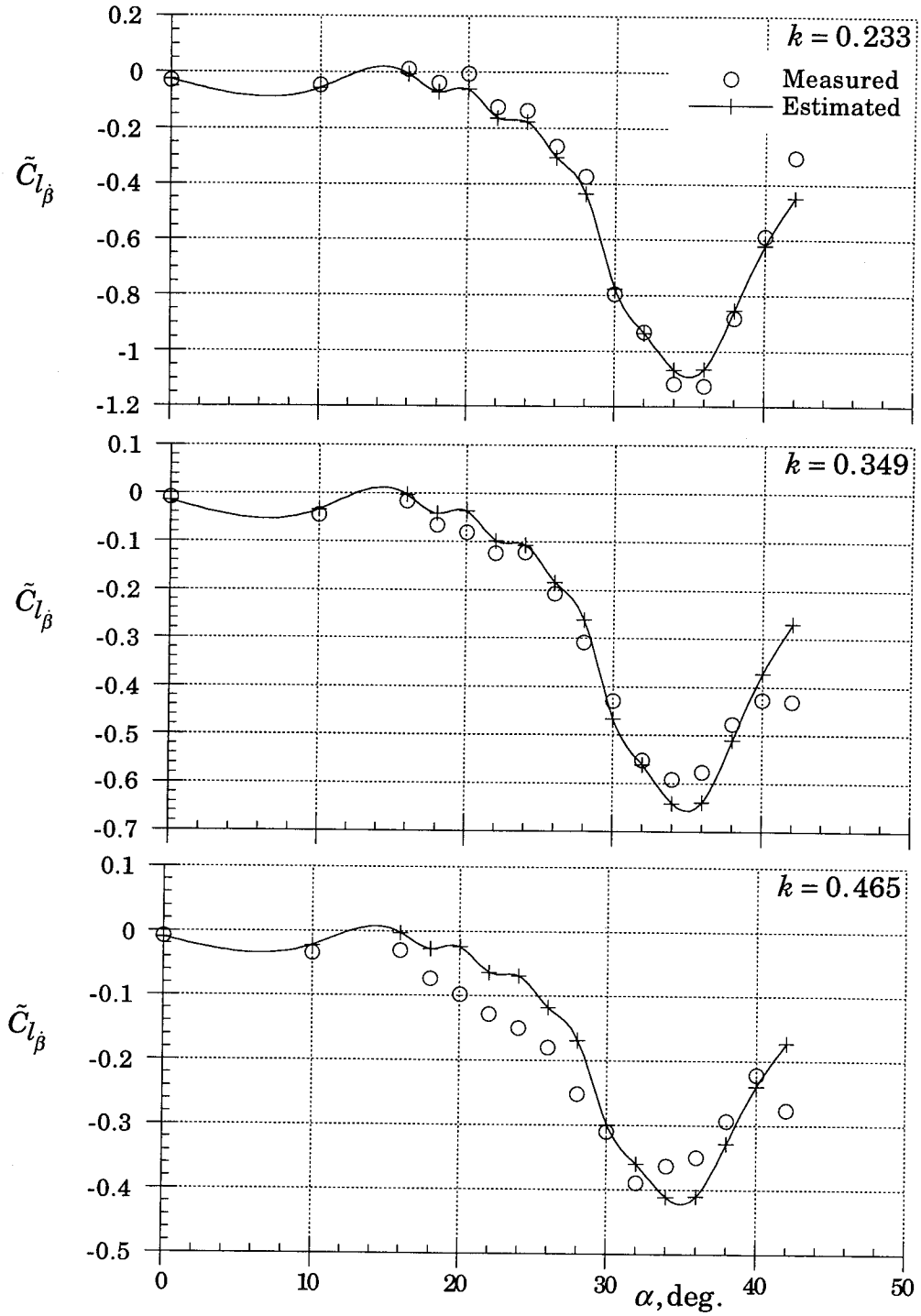

Figure 18. Measured and estimated out-of-phase components of rolling moment. In-sideslip oscillations of HIRM 2, canard off.

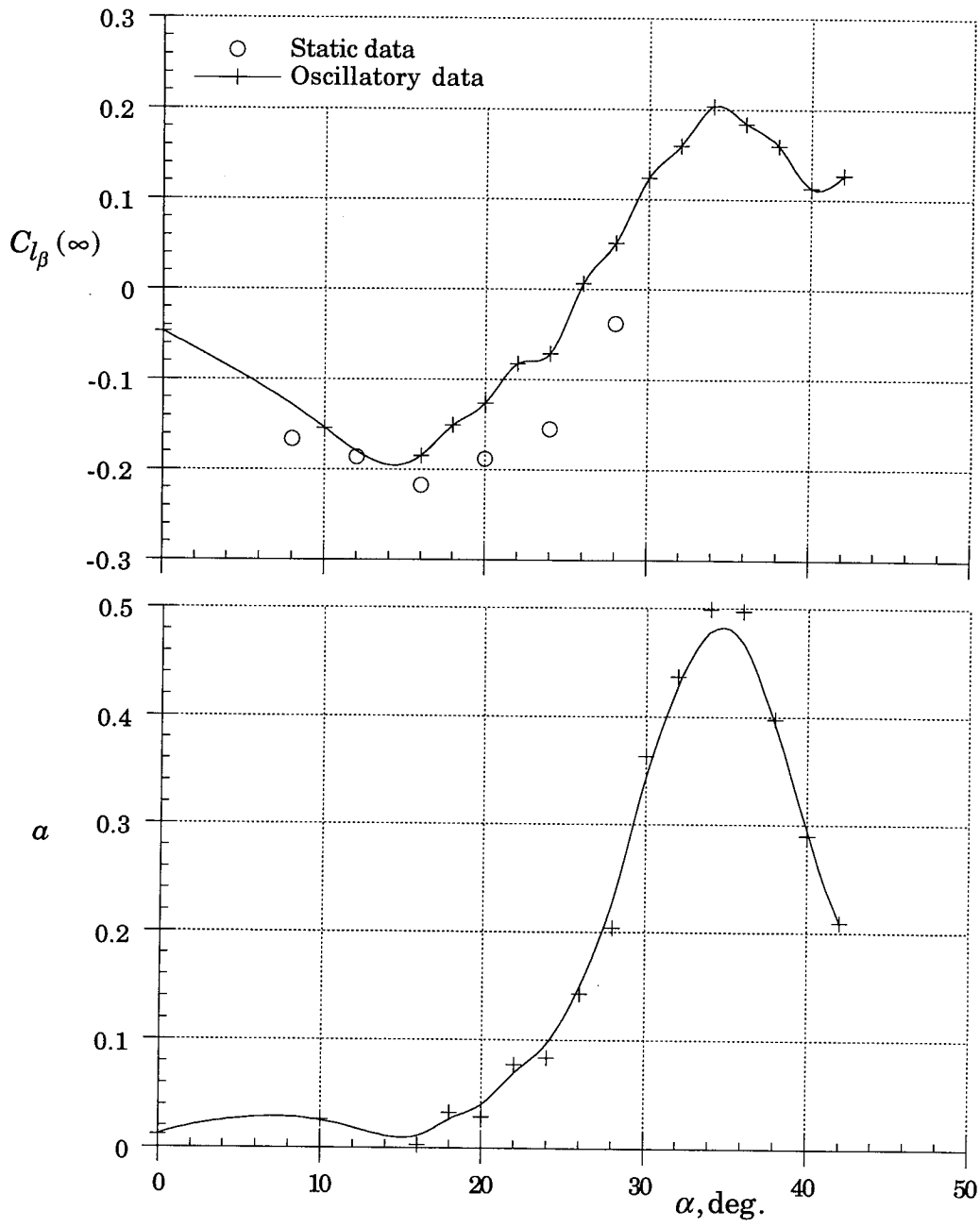

Figure 19. Estimated parameters of rolling moment components. Insideslip oscillations of HIRM 2, canard off.

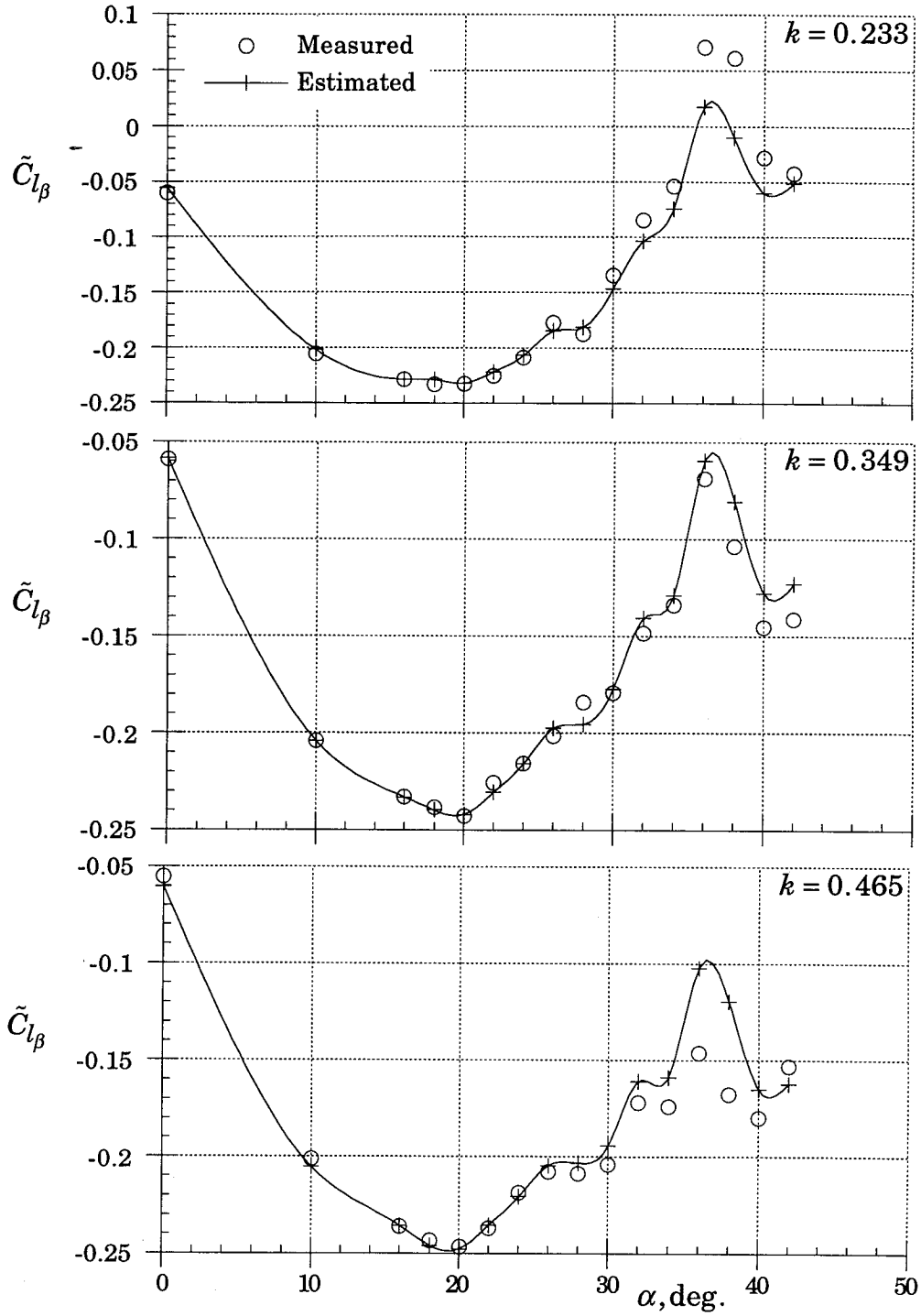

Figure 20. Measured and estimated in-phase components of rolling moment. In-sideslip oscillations of HIRM 2, canard at 0°.

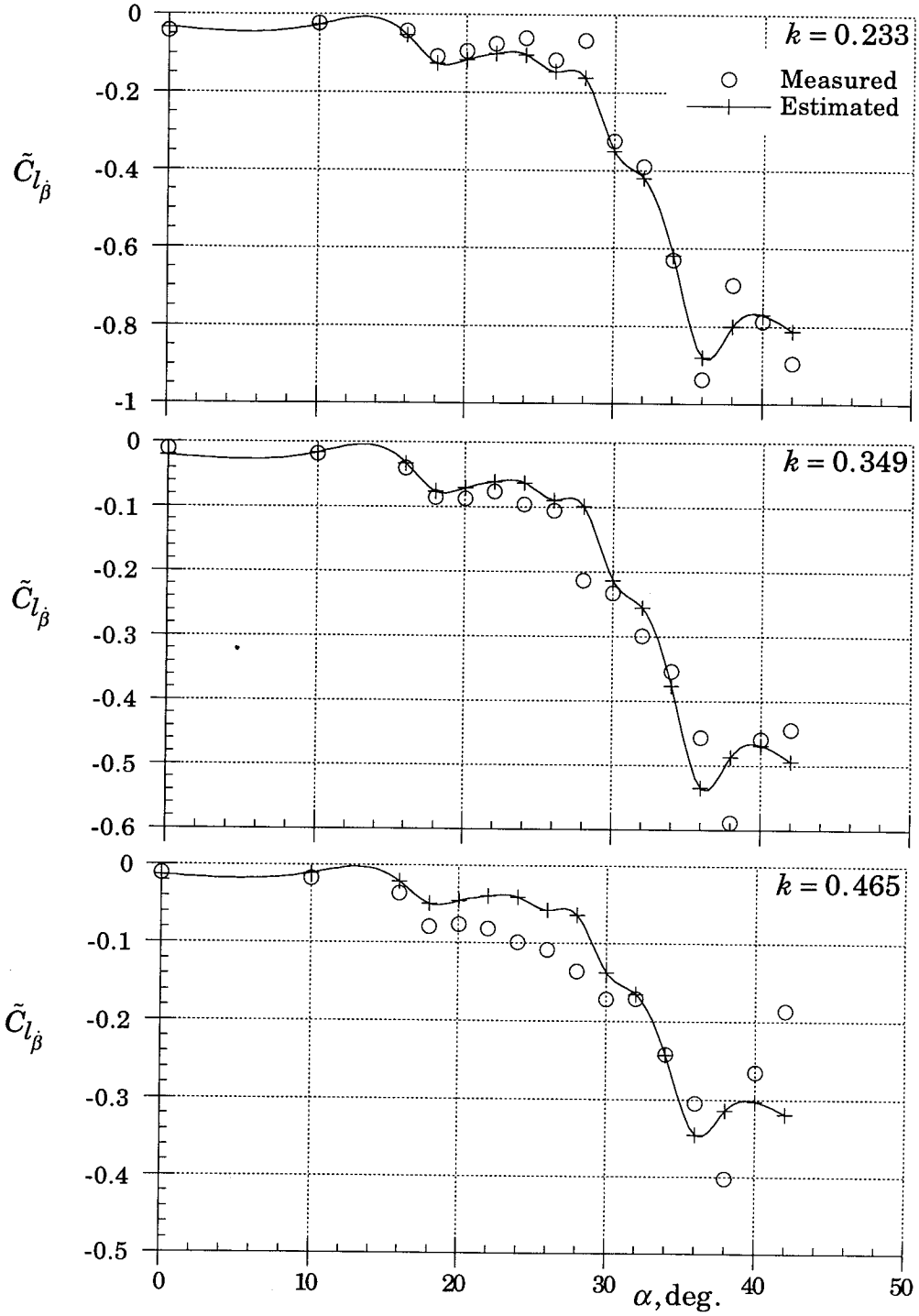

Figure 21. Measured and estimated out-of-phase components of rolling moment. In-sideslip oscillations of HIRM 2, canard at 0°.

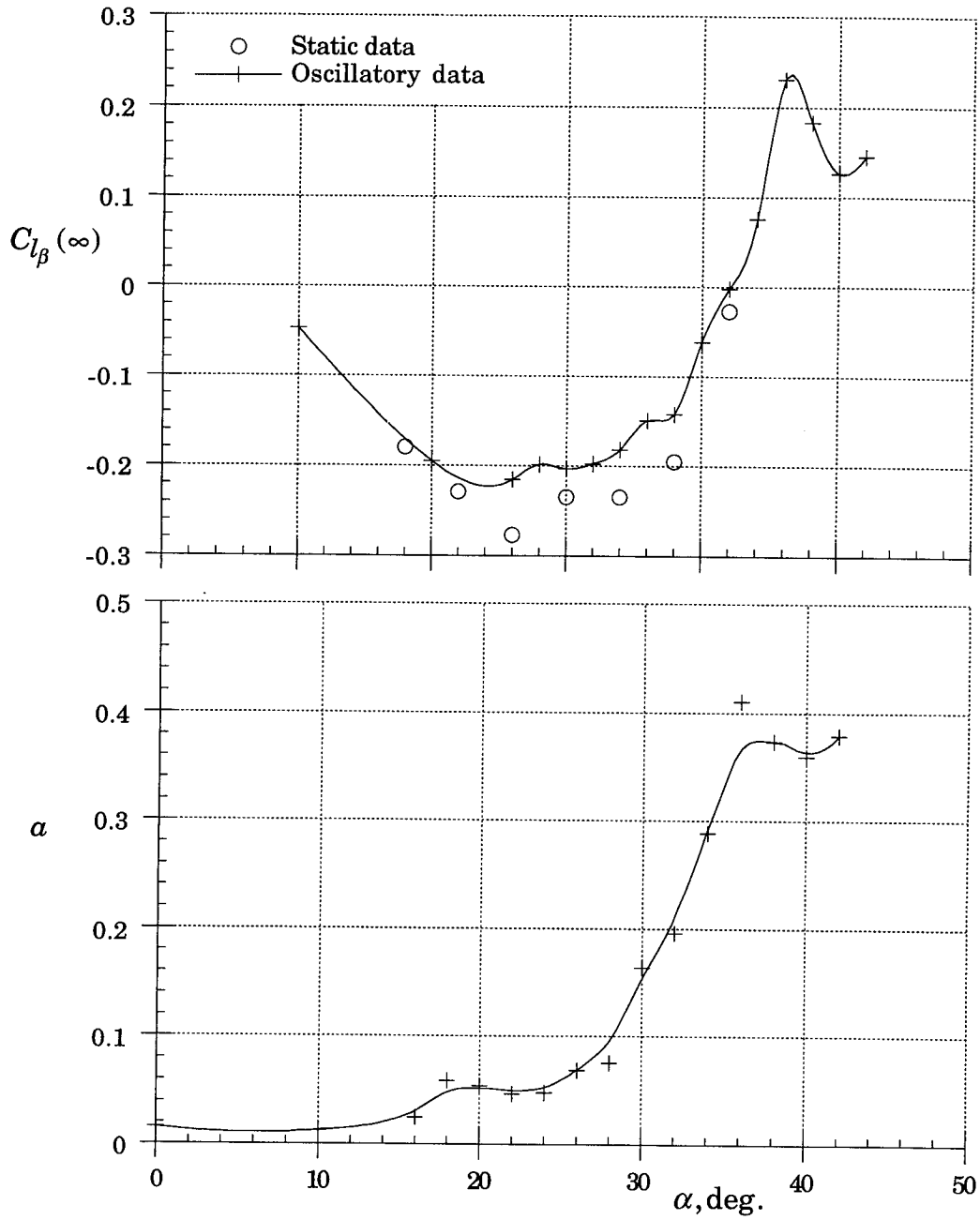

Figure 22. Estimated parameters of rolling moment components. Insideslip oscillations of HIRM 2, canard at 0°.

REPORT DOCUMENTATION PAGE

Form Approved
OMB No. 0704-0188

1. AGENCY USE ONLY (*Leave blank*)	2. REPORT DATE	3. REPORT TYPE AND DATES COVERED
	April 1995	Technical Memorandum

4. TITLE AND SUBTITLE
Modeling of Aircraft Unsteady Aerodynamic Characteristics
Part 2 - Parameters Estimated from Wind Tunnel Data

5. FUNDING NUMBERS
505-64-52-01

6. AUTHOR(S)
Vladislav Klein and Keith D. Noderer

7. PERFORMING ORGANIZATION NAME(S) AND ADDRESS(ES)
NASA Langley Research Center
Hampton, VA 23681-0001

8. PERFORMING ORGANIZATION REPORT NUMBER

9. SPONSORING / MONITORING AGENCY NAME(S) AND ADDRESS(ES)
National Aeronautics and Space Administration
Washington, DC 20546-0001

10. SPONSORING / MONITORING AGENCY REPORT NUMBER
NASA TM - 110161

11. SUPPLEMENTARY NOTES
Klein and Noderer: The George Washington University, Joint Institute for Advancement of Flight Sciences, Langley Research Center, Hampton, Virginia.

12a. DISTRIBUTION / AVAILABILITY STATEMENT
Unclassified-Unlimited

Subject Category 08

12b. DISTRIBUTION CODE

13. ABSTRACT (*Maximum 200 words*)

Aerodynamic equations with unsteady effects were formulated for an aircraft in one-degree-of-freedom, small-amplitude, harmonic motion. These equations were used as a model for aerodynamic parameter estimation from wind tunnel oscillatory data. The estimation algorithm was based on nonlinear least squares and was applied in three examples to the oscillatory data in pitch and roll of 70° triangular wing and an X-31 model, and in-sideslip oscillatory data of the High Incidence Research Model 2 (HIRM 2). All three examples indicated that a model using a simple indicial function can explain unsteady effects observed in measured data. The accuracy of the estimated parameters and model verification were strongly influenced by the number of data points with respect to the number of unknown parameter.

14. SUBJECT TERMS
Wind tunnel testing, Aerodynamic model equations, Unsteady aerodynamics, and Indicial functions

15. NUMBER OF PAGES
42

16. PRICE CODE
A03

17. SECURITY CLASSIFICATION OF REPORT	18. SECURITY CLASSIFICATION OF THIS PAGE	19. SECURITY CLASSIFICATION OF ABSTRACT	20. LIMITATION OF ABSTRACT
unclassified	unclassified	unclassified	